The Higgs boson implications and prospects for future discoveries

Steven D. Bass[1,2]✉, *Albert De Roeck*[3,4]✉ *and Marumi Kado*[5,6]✉

Abstract | The Higgs boson, a fundamental scalar boson with mass 125 GeV, was discovered at the Large Hadron Collider (LHC) at CERN in 2012. So far, experiments at the LHC have focused on testing the Higgs boson's couplings to other elementary particles, precision measurements of the Higgs boson's properties and an initial investigation of the Higgs boson's self-interaction and shape of the Higgs potential. The Higgs boson mass of 125 GeV is a remarkable value, meaning that the underlying state of the Universe, the vacuum, sits very close to the border between stable and metastable, which may hint at deeper physics beyond the standard model. The Higgs potential also influences ideas about the cosmological constant, the dark energy that drives the accelerating expansion of the Universe, the mysterious dark matter that comprises about 80% of the matter component in the Universe and a possible phase transition in the early Universe that might be responsible for baryogenesis. A detailed study of the Higgs boson is at the centre of the European Strategy for Particle Physics update. Here we review the current understanding of the Higgs boson and discuss the insights expected from present and future experiments.

Vacuum expectation value
The matrix element of a field or operator in the vacuum.

Higgs condensate
The Bose–Einstein condensate of Higgs bosons, which forms in the vacuum.

[1]*Kitzbühel Centre for Physics, Kitzbühel, Austria.*

[2]*Jagiellonian University, Marian Smoluchowski Institute of Physics, Kraków, Poland.*

[3]*CERN, Experimental Physics Department, Geneva, Switzerland.*

[4]*University of Antwerp, Physics Department, Antwerp, Belgium.*

[5]*INFN Sezione di Roma and Dipartimento di Fisica, Sapienza Universitá di Roma, Rome, Italy.*

[6]*IJCLab, Université Paris-Saclay, CNRS/IN2P3, Orsay, France.*

✉*e-mail:* *Steven.Bass@cern.ch*; *Albert.De.Roeck@cern.ch*; *Marumi.Kado@cern.ch*

https://doi.org/10.1038/s42254-021-00341-2

The discovery of the Higgs boson in 2012 at CERN's Large Hadron Collider (LHC) by the ATLAS[1] and CMS[2] experiments was a milestone for particle physics, recognized by the award of the 2013 Nobel Prize for Physics to François Englert[3] and Peter Higgs[4]. The Higgs boson is central to our understanding of particle physics. It is the first (and so far only) discovered (seemingly) elementary particle with spin zero.

The standard model (SM) of particle physics[5–7] provides an excellent description of particle physics experimental results so far, from collider experiments at the LHC[8], with centre-of-mass energy up to 13 TeV, to low-energy precision measurements, including those of the fine structure constant[9,10], of quantum electrodynamics and of the electron's electric dipole moment[11].

Everyday matter consists of elementary fermions: quarks and leptons. Particle interactions are determined by local gauge symmetries and mediated by the exchange of spin-one gauge bosons. These are the massless photons in quantum electrodynamics, which bind electrons to nuclei in atoms, the gluons in quantum chromodynamics (QCD), which bind quarks inside the proton, and the massive W and Z bosons for the weak interactions that power the Sun and nuclear reactors. In the SM, symmetry drives the particle interactions with invariance under local changes in the phases of fermion fields. An important ingredient of the theory is the origin of particle masses. Within the SM the masses of the W and Z gauge bosons and charged fermions emerge from coupling of these particles to the scalar spin-zero Higgs field, which comes with a non-vanishing vacuum expectation value (VEV), and a Higgs condensate filling all space.

Although the discovered boson behaves very much like the SM Higgs with a mass of 125 GeV, in which case it completes the particle spectrum of the SM, important open questions remain, connecting particle physics to cosmology, that require new physics to answer. These relate to the nature of the dark energy that drives the accelerating expansion of the Universe[12], the origin of the matter–antimatter asymmetry in the Universe[13], primordial inflation[14] and the mysterious extra dark matter that comprises about 80% of the matter component in the Universe[15]. A considerable amount of theoretical work has gone into investigating possible connections between these open questions and the properties of the Higgs boson. The Higgs boson's observed decays to vector bosons indicate the existence of a Higgs condensate. Although its mass was expected to be commensurate with the electroweak scale to ensure the unitarity of the scattering of longitudinally polarized vector bosons, such a relatively small mass (which is much less than the Planck scale that defines the limit of particle physics before quantum gravity effects might appear) raised the fundamental question of the naturalness of the SM.

The European Particle Physics Strategy[16,17] identified precision studies of the Higgs boson as the main priority for the next high-energy collider with measurements first at the planned high-luminosity upgrade of the LHC and, later, with a dedicated Higgs factory as a new

Key points

- The discovery of the Higgs boson was a major milestone in particle physics, confirming the standard model.
- Direct tests of the couplings of the Higgs boson to fermions confirmed the mechanism that gives mass to the W and Z bosons, thus making the electroweak interaction short range. A recent highlight is the direct observation of the Higgs boson coupling to muons.
- The observed properties of the Higgs boson put the standard model vacuum intriguingly close to the border between stable and metastable. Further connections to the open questions pertaining to baryogenesis, the nature of dark matter and dark energy and cosmic inflation mean that the Higgs boson is central to our understanding of the Universe.
- Precision measurements of the Higgs boson to further probe its interactions and possible deeper origin and structure are an essential part of the High-Luminosity Large Hadron Collider programme and were recently identified by the European Strategy for Particle Physics to be the highest priority for the next high-energy collider facility.

facility. This programme involves essential interaction between experiment and theory.

This Review surveys the Higgs boson physics with an outlook to future experiments. We start by discussing the role of the Higgs boson in the origin of mass, then review the discovery and early measurements of the Higgs boson's properties and continue with the Higgs coupling to fermions. Next, we summarize the status of measurement of the Higgs boson's properties and interactions in comparison with the predictions for the Higgs boson described by the SM. We discuss Higgs self-coupling and then focus on searches for any extra Higgs states or possible new charge-parity (CP) violation in the Higgs sector. We describe open theoretical issues connected to the Higgs boson in particle physics and cosmology and we end with a description of future measurements that might shed light on these questions and the role of the Higgs in understanding the deep structure of the Universe.

Higgs boson and massive gauge bosons

The Higgs story begins with the interplay between mass and gauge invariance. Taken alone, mass terms for gauge bosons break the underlying gauge symmetry. For example, consider particles (fermions or scalar bosons) χ interacting with a spin-one gauge field $\mathbf{A}_\rho$ with the system invariant under the local gauge transformations $\chi \rightarrow e^{i\omega}\chi$ and $\mathbf{A}_\rho \rightarrow \mathbf{A}_\rho + \frac{1}{g}\partial_\rho\omega$. Here ω is the gauge symmetry parameter, $\partial_\rho = \frac{\partial}{\partial x^\rho}$ is a partial derivative, and g is the coupling of $\mathbf{A}_\rho$ to χ; ρ denotes the Lorentz index. Introducing a mass term $m^2\mathbf{A}_\rho\mathbf{A}^\rho$ violates the gauge symmetry without extra ingredients.

This problem is resolved through the Brout–Englert–Higgs (BEH) mechanism (see REFS[18–21] and related work in REFS[22,23]). The gauge symmetry of the underlying theory can be hidden in the ground state. The symmetry parameter ω freezes out to a particular value, with all possible values being degenerate. This process, known as spontaneous symmetry breaking, generates massless Goldstone modes — one for each generator of the symmetry. For local gauge symmetries these massless Goldstone modes combine with the gauge bosons to generate new longitudinal modes of the gauge fields, conserving the total number of degrees of freedom. The transverse and longitudinal components of the spin-one gauge field acquire non-zero mass, which is the same for both components. In addition, a new scalar boson is produced with finite coupling to the massive gauge fields — the Higgs boson.

In the SM of particle physics, besides giving mass to the W and Z gauge bosons, the BEH mechanism also has a vital role, ensuring a consistent very high-energy behaviour of scattering amplitudes. The Higgs boson, with mass 125 GeV, guarantees the unitarity of high-energy collisions involving massive W and Z bosons, with the Higgs boson cancelling terms from the longitudinal component of the W and Z bosons that would otherwise violate perturbative unitarity (meaning that scattering probabilities calculated using Feynman diagrams would grow larger than one)[24–27]. The Higgs boson is also essential for the renormalizability of the theory, namely to ensure a consistent treatment of the ultraviolet divergences, which appear in Feynman diagrams involving loops[28–30].

To understand the BEH mechanism, consider the coupling of the gauge field $\mathbf{A}_\rho$ to a complex scalar field ϕ via the gauge covariant derivative with coupling constant g, namely $D_\rho\phi = [\partial_\rho + ig\mathbf{A}_\rho]\phi$. Under the local gauge transformation $\phi \rightarrow e^{i\omega}\phi$, $D_\rho\phi \rightarrow e^{i\omega}D_\rho\phi$ with the partial derivative acting on ω compensated by the gauge transformation of A_ρ.

The scalar field is taken with potential:

$$V(\phi) = \frac{1}{2}\mu^2\phi^2 + \frac{1}{4}\lambda\phi^4. \quad (1)$$

Here the self-coupling $\lambda \geq 0$ so the potential has a finite minimum, as required for vacuum stability.

If $\mu^2 > 0$ the potential describes a particle with mass μ. When $\mu^2 < 0$ the potential has a minimum at:

$$|\phi| \equiv \frac{v}{\sqrt{2}} = \sqrt{-\frac{\mu^2}{2\lambda}}. \quad (2)$$

This potential is illustrated in FIG. 1. Excitations around the degenerate minima of the potential — the bottom of the 'Mexican hat' shape — correspond to a massless Goldstone mode. Gauge freedom allows us to choose v as the VEV of the real part of ϕ with all choices of vacuum state being degenerate and physically equivalent. Expanding the scalar field about this minimum of the potential, the Goldstone mode is 'eaten' to become the longitudinal mode of $\mathbf{A}_\nu$, which now acquires mass g^2v^2. The Higgs boson H with mass squared $m_H^2 = 2\lambda v^2$ corresponds to excitations up the rim of the potential.

The consistency of massive gauge bosons with gauge invariance was first solved by Philip W. Anderson[31] in the context of massive 'photons', called plasmons, in superconductors[31]. The photon behaves as a wave on a sea of Bardeen–Cooper–Schrieffer (BCS) Cooper pairs, which in this case act as the scalar field ϕ, condensing in the ground state. The order parameter is not rigid with zero momentum Cooper pairs, but fluctuates in the longitudinal component to preserve the translational symmetry of the electron gas. The plasmon's transverse component is a modification of a real photon propagating in the plasma, whereas the longitudinal mode is an

Naturalness
The theoretical idea that dimensionless ratios of mass scales in a physical theory should be of order one. That is, without fine tuning, a mass parameter can only be much smaller than the others if setting it zero increases the symmetry of the theory.

Gauge freedom
With gauge symmetry, we are free to choose the gauge symmetry parameters to make the physics look simplest, with all choices of gauge parameters being physically equivalent and degenerate.

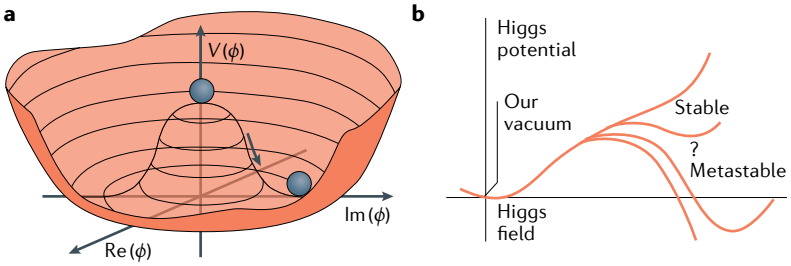

Fig. 1 | **The Higgs potential and its sensitivity to quantum corrections. a** | The Higgs potential $V(\phi)$ for the scalar field ϕ for mass parameter $\mu^2 < 0$; see equation (1). Choosing any of the points at the bottom of the potential spontaneously breaks the rotational U(1) symmetry. **b** | Quantum corrections can change the shape of the Higgs potential. Here the minimum of "our vacuum" is taken at $|\phi| = \frac{v}{\sqrt{2}}$ with $v = 246$ GeV. When quantum corrections to standard model couplings are included, the vacuum may develop a second minimum, leading to vacuum metastability. Panel **a** © 2015–2021 CERN (License: CC-BY-4.0). Panel **b** reprinted with permission from REF.[208], APS Physics.

attribute of the system. Massive plasmons are manifest through the exponential decrease of the magnetic field inside the superconductor (the Meissner effect).

The extension of this physics to relativistic dynamics[18–21] has been introduced to provide a consistent model of weak interactions in particle physics[32–35]. Contrary to the BCS case, the weak interaction requires the introduction of an additional fundamental scalar field. A dynamic explanation of the Higgs mechanism using BCS theory would be a major breakthrough and is one of the fundamental motivations to measure with the highest possible precision the properties of the Higgs particle. For a more detailed history of theoretical developments, see REF.[36].

For weak interactions the gauge group is SU(2). There are three massless Goldstone modes, which combine to form the massive W charged bosons and the massive Z. The massless photon and neutral Z boson are linear combinations of the neutral weak SU(2) gauge boson and a U(1) gauge boson called hypercharge. Within the SM, the BEH mechanism is also important for the fermion masses, something required by parity violation of weak interactions[37]. The weak interaction gauge bosons couple to SU(2) doublets of left-handed leptons and quarks, whereas right-handed fermions are weak interaction neutral. Singlet mass terms for the charged fermions are constructed by contracting the left-handed fermion doublets with the SU(2) Higgs doublet, including the VEV, and then multiplying by the right-handed fermion. The SM particle masses are:

$$m_W^2 = \frac{1}{4}g^2v^2, \quad m_Z^2 = \frac{1}{4}(g^2 + g'^2)v^2,$$
$$m_f = y_f\frac{v}{\sqrt{2}}, \quad m_H^2 = 2\lambda v^2. \tag{3}$$

Here g and g' are the SU(2) and U(1) gauge couplings and y_f denotes the fermion Yukawa coupling to the Higgs boson. Without considering the tiny neutrino masses, the SM has 18 parameters: 3 gauge couplings and 15 in the Higgs sector (6 quark masses, 3 charged leptons, 4 quark mixing angles including 1 CP-violating complex phase, the W and Higgs masses). There is a wide range of masses with $m_W = 80$ GeV, $m_Z = 91$ GeV, $m_H = 125$ GeV and the charged fermion masses ranging from 0.5 MeV for the electron up to 173 GeV for the top quark. The Higgs VEV $v = 246$ GeV. In natural units $v = (\sqrt{2}\,G_F)^{-\frac{1}{2}}$, where G_F is the Fermi coupling constant of weak interactions.

Small changes in the Higgs couplings and particle masses can lead to a very different Universe, assuming that the vacuum remains stable. One example is that small changes in the light-quark masses can prevent Big Bang nucleosynthesis[38]. Once radiative corrections are taken into account, the stability of the Higgs vacuum is very sensitive to the value of the top quark mass. Vitally, the Higgs boson cannot be too heavy to do its job of maintaining perturbative unitarity. If the Higgs boson had not been found at the LHC, new strong dynamics would have been needed in the energy range of the experiments, for example, involving strongly interacting W^+W^- scattering with the Higgs boson replaced by some broad resonance in the WW system[39].

In contrast to particle physics, where the Higgs boson is treated as an elementary particle, in condensed matter systems, the Higgs boson forms as a collective mode[40]. Following the Higgs boson discovery in high-energy physics, collective Higgs states have been observed in superconductors[41]; for discussion see REFS[42–44].

Discovery and first measurements

More than 40 years after the original postulation of the electroweak symmetry breaking through the BEH mechanism, the first potential experimental observation of its predictions was announced by the ATLAS and CMS experiments on 4 July 2012. The LHC is a circular particle accelerator, colliding proton beams at centre-of-mass energies of 7 TeV and 8 TeV (in run 1, 2010–2012) and 13 TeV (in run 2, 2015–2018) to search for new particles and phenomena[45]. The ATLAS[46] and CMS[47] experiments are two general-purpose detectors making use of the highest luminosities (high rates of collision events) at the LHC.

The announcement from ATLAS and CMS was based on the data collected in run 1, which was sufficient for both experimental collaborations to claim independently the observation of a new particle, that is, with a significance of the result of more than five standard deviations, or 5σ, away from a background-only result, meaning that the chance of this result being due to a fluctuation of the background is less than 1 in 3,500,000. Measurements that give a significance above 3σ are considered as evidence.

According to the SM, a Higgs boson with mass about 125 GeV produced in a proton–proton collision has a lifetime of only about 1.6×10^{-22} seconds, after which it disintegrates into particles that are recorded by the detectors. The 2012 ATLAS and CMS data showed that the new particle had a mass of around 125 GeV (about 133 times the mass of a proton) and decayed into vector bosons, namely a pair of photons, W bosons or Z bosons, exactly as predicted by the SM theory, and therefore was labelled 'a Higgs boson candidate'. The observed decay into two photons meant that the new particle could not have spin one, according to the Landau–Yang

Radiative corrections
Quantum fluctuations in the intermediate state of the particle interactions.

theorem[48,49]. In the SM the Higgs boson has no electric charge of its own and decays into two photons via a fermion or W boson loop.

A few months after the initial announcement, a next crucial step was made by verifying the quantum properties of the new particle, demonstrating that it had to be a scalar spin-zero particle, as required for the messenger of the BEH field. Although some small-level mixing with a CP-odd component is still possible, the new particle has been firmly excluded from being a pure CP-odd state[50–52]. (Discrete CP symmetry refers to the joint action of charge conjugation invariance, changing particles for antiparticles, and parity reversal. The SM Higgs boson is a scalar, transforming as a CP-even state under CP transformations.) This result promoted the particle to 'a Higgs boson'. However, it is still possible that the new particle might not be the SM Higgs boson, but a look-alike, such as a scalar particle from an extended theory sector or even a composite particle. For further insight, the Higgs boson properties have to be mapped out in detail, which at present can only be done at the LHC. One needs to answer the extra questions: does this new particle also couple to the other known fundamental particles as expected, for example the quarks and charged leptons? What is the exact mass value and width of this resonance? Is it possible to measure the shape of the Higgs field potential directly, for example, via Higgs boson pair production?

ATLAS and CMS discovered this new particle with a data sample of about 10 inverse femto barn (fb^{-1}) each. An additional 15 fb^{-1} was collected by the end of 2012 by both experiments in run 1. From 2015 to 2018, in the LHC run 2, the experiments collected 139 fb^{-1} each at a higher centre-of-mass energy of 13 TeV. In the next few years the LHC will deliver, for each experiment, approximately 150 fb^{-1} in run 3 (scheduled for 2022–2024), and then the accelerator and both experiments will be upgraded for the high-luminosity phase to collect a total of 3–4 inverse attobarn (ab^{-1}) each.

Many analyses of the collected dataset from run 2 are still being finalized, but several full run 2 results have been completed and show an emerging picture that we will discuss in the next sections. In the collisions data from this run, about 7 million Higgs bosons have been produced, so the LHC can be considered to be the first 'Higgs factory', even though only a fraction could be identified and used to study its properties. LHC data analysis proceeds in parallel with advances in precision theoretical calculations for the SM production and decay rates as well as modelling of the backgrounds[53–56].

In the SM all the couplings of the Higgs boson to fermions and vector bosons were known as a function of the Higgs boson's mass even before the discovery of the Higgs boson. The only parameter that was not predicted by the theory was the mass of the Higgs boson itself. Upper bounds had been obtained from the unitarity in longitudinal vector boson scattering, which was an essential argument that the LHC should be able to observe either the Higgs boson or signs of new underlying strong dynamics in the teraelectronvolt (TeV) range. This idea is referred to as the no-lose theorem. A 95% confidence level upper bound on the Higgs boson mass of 166 GeV had already been derived from previous electoweak measurements, mainly from the former Large Electron–Positron (LEP) collider at CERN[57].

To measure the mass of the Higgs boson, its decay into a pair of photons or Z bosons, with each Z boson itself decaying into a pair of electrons or muons, constitutes the best channels to use, because charged leptons and photons can be measured with excellent precision by the LHC detectors and thus the mass of the Higgs boson can be fully determined from the invariant mass of the final-state particles. The resulting mass distributions show typical resonant structures in which the width of the resonance is determined by the detector resolution. The extracted central mass value for the Higgs boson from the combined ATLAS and CMS run 1 measurements was reported in REF.[58] to be $125.09 \pm 0.21 \pm 0.11$ GeV. Subsequently new values for the mass were reported by CMS to be 125.38 ± 0.14 GeV (REF.[59]) and by ATLAS to be 124.97 ± 0.24 GeV (REF.[60]), with these measurements using both the diphoton and ZZ decay channels. It is remarkable that, in less than a decade, the mass of this particle is already known to a precision of almost one per mille.

Interestingly, the mass of 125 GeV is ideal for a detailed experimental study of this new particle. Indeed, the product of the branching ratios of the SM Higgs boson in all decay channels available below the top-antitop threshold has been reported in REF.[61] to be a Gaussian distribution of the Higgs boson mass with a maximum centred at $m_H \approx 125$ GeV, that is, exactly at the mass value where the new boson has been discovered. No other SM Higgs boson mass value has a better combined signal strength for the whole set of decay channels. Conversely, this mass value still allows for many beyond-the-SM scenarios.

Higgs boson couplings to fermions

To discover the Higgs boson, physicists searched for the footprints of the particles it decays to, more precisely, channels where it decays to charged fermions as well as gauge bosons. The observed inclusive production rate of the boson, that is, for its production along with any other final-state particles, confirmed that the predicted main production process should be through gluon fusion: $gg \rightarrow H$. This process indirectly implied that the Higgs boson should couple to top quarks, which are involved in the decay quantum loop. However, direct evidence of the coupling of the Higgs boson to fermions is needed to demonstrate that the minimal version of the SM is correct and that the same scalar field is responsible for the masses of the vector bosons and the charged fermions.

Such a direct test of the SM would be to establish the decay of the Higgs boson into charged fermions, and was a key physics target for the LHC run 2. Decays to all fermions are kinematically allowed except for the decay into a top plus anti-top quark pair. An important check is the quantitative comparison of the coupling strengths to the different fermions, which for the quantum particle associated with the BEH field in the SM are expected to be proportional to the masses of the respective fermions.

The most easily accessible channels are decays to the bottom or b-quarks and to the tau leptons, members of

Barn
A unit that quantifies the integrated luminosity. It has the dimension of inverse area, proportional to the amount of proton–proton collisions produced by the Large Hadron Collider (LHC). One femtobarn 1 fb = 10^{-43} m^2. One inverse attobarn 1 ab^{-1} = 10^3 fb^{-1}. One inverse femtobarn corresponds to approximately 10^{14} proton–proton collisions in the LHC.

Signal strength
The ratio of the signal rate divided by the predicted rate for a standard model (SM) Higgs boson at a given mass, denoted by the symbol μ_S. The closer μ_S is to one, the more it resembles a SM Higgs boson.

Diphoton channel
(Higgs) particle production with two photons in the final state.

the third and most massive fermion generation. First evidence for decays to the third fermion generation, tau leptons and b-quarks, has been reported already from the run 1 data. The couplings to the second fermion generation, the muon and the charm and strange quarks, are more challenging. The LHC is unlikely to be able to test couplings to the first generation with the present methods, and such a test remains the aim of a future, very intense Higgs factory.

Below, we focus on the Higgs boson coupling to the top quark. This is special because the top quark is heavier than the Higgs boson and its Yukawa coupling to the Higgs boson is $y_t \approx 1$. Next, we will discuss measurements of the Higgs boson couplings to the tau lepton, the bottom quark and the lighter mass fermions, including a recent experimental highlight: observation of the Higgs boson to muon coupling.

The Higgs boson to top quark Yukawa coupling. The top quark is the heaviest known fundamental fermion in nature; its measured mass[62] of 172.76 ± 0.30 GeV means that the top quark Yukawa coupling is very large, strikingly close to one. The precise measurement of this coupling plays an essential part in the energy-scale dependence of the Higgs boson self-coupling, which in turn is essential to understanding the stability of the particle physics Higgs vacuum: does the current VEV of the BEH field correspond to the real minimum of the Higgs potential?

The Yukawa coupling of the Higgs boson to the top quark also allows for a fundamental check of the quantum consistency of the theory by comparison with indirect measurement through the main gluon fusion production process discussed above, which necessarily proceeds through quantum loop corrections and is therefore potentially sensitive to contributions from other, yet unobserved, states.

A direct measurement can be made through the associated production of the Higgs boson with a pair of $t\bar{t}$ (top plus antitop) quarks. The topologies of such events (the combination of particle interactions leading to them) are complex and typically contain many jets, among which two at least originate from b-quarks, electrons or muons, and the decay products of the Higgs boson itself; see FIG. 2a. The first direct observation of the Yukawa coupling of the Higgs boson to the top quark was achieved only with a large, but partial, run 2 dataset and using all Higgs boson decay channels $b\bar{b}$, $\tau^+\tau^-$, WW^*, ZZ^* and $\gamma\gamma$ by ATLAS and CMS[63,64]. The respective signal strengths for $t\bar{t}H$ production were found to be 1.32 ± 0.39 (ATLAS) and 1.26 ± 0.31 (CMS), in agreement with the SM expectation.

With the entire dataset, the diphoton channel alone provides an unambiguous observation of the $pp \rightarrow t\bar{t}H$ production process[65,66]; see FIG. 2b. The other Higgs boson decay channels are more challenging for precision measurements and improving their sensitivity relies on progress in the theoretical predictions for the backgrounds.

The presence of the Higgs boson with a large top-quark Yukawa coupling can also be indirectly measured through production processes where the Higgs boson does not appear in the final state, but contributes as an exchange particle in the intermediate state of the reaction. These indirect measurements have been carried out in top-pair production processes, including the spectacular four-top channel for which first evidence has been observed, but are so far not competitive with the constraints from the direct observation of the associated production of a Higgs boson with a top-quark pair.

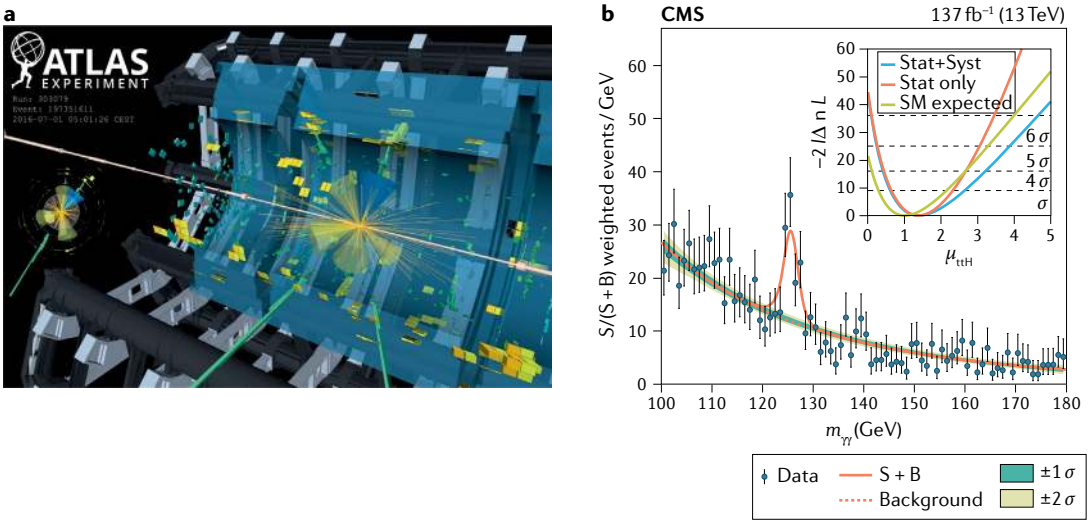

Fig. 2 | **Top quark production in Higgs boson decays. a** | A 3D event display of a candidate $H \rightarrow \gamma\gamma$ in the $pp \rightarrow t\bar{t}H$ production mode, exemplifying the complex topologies of events where in addition to the two isolated photons (in green in the lower part of the detector), six jets are present, among which one is tagged as originating from a b-quark (blue cone). **b** | The distribution of the invariant mass of the diphoton system ($m_{\gamma\gamma}$) for events selected in $t\bar{t}H$-specific topologies. The inset in the figure also displays the measurement's likelihood as a function of the strength of signal, indicating the subdominant impact of systematic uncertainties in this channel. SM, standard model; Stat, statistical error; Syst, systematic error; S, signal; and B, background. Panel **a** photograph: ATLAS Collaboration; copyright: CERN; panel **b** reprinted from REF.[65], CC BY 4.0.

The single production of a single top quark together with a Higgs boson has also been searched for in the experiments. This process is especially interesting[67] since it is sensitive to the sign of the top-quark Yukawa coupling y_t through the tree-level interference between the production through the Higgs boson emission by a top quark and a W boson[68]. For SM-like couplings of the Higgs boson to W and Z bosons, CMS data[69] with 36 fb^{-1} favours positive values of y_t and excludes negative values below $-0.9y_t^{SM}$. Combined measurements with integrated luminosity of 137 fb^{-1} of $t\bar{t}H$ and tH production in final states with electrons, muons and hadronically decaying tau leptons yield constraints on $\kappa_t = y_t/y_t^{SM}$ in the range $-0.9 < \kappa_t < -0.7$ or $0.7 < \kappa_t < 1.1$ (REF.[70]).

The Higgs boson coupling to tau leptons. Tau leptons have a mass of 1.777 GeV and for a SM Higgs boson of 125 GeV, the decay rate, or branching ratio, into a $\tau^-\tau^+$ lepton pair is about 6.3%. Tau leptons are unstable, though, and decay with a mean lifetime of about 10^{-13} seconds, as observed at the LHC, into a narrow low-multiplicity hadronic jet (that is, a jet carrying few particles), or a muon or electron, and in all cases in association with one or more neutrinos, which go undetected in the experiments. The experiments have developed refined τ-tagging methods in the data for the most important τ decay channels, and have also been using additional event activity characteristics apart from the Higgs boson production to master and control the large backgrounds from non-Higgs boson production processes. During run 1, the Higgs boson to $\tau^-\tau^+$ decay was established by both experiments with a significance of about 3σ for CMS and 4.5σ for ATLAS[71,72] with the 5σ threshold already crossed in run 1 by the ATLAS and CMS combination[73].

Results based on partial run 2 data confirm these results and have established an observation of the Higgs boson to $\tau^-\tau^+$ decay channel. CMS combined results of several production channels measured with 36 fb^{-1} of data and produced the overall result of an observation of the Higgs boson decaying into a $\tau^-\tau^+$ pair with a significance of 5.5σ and signal strength for a SM Higgs boson μ_S of $1.24^{+0.29}_{-0.27}$ from run 2 data[74] or 0.98 ± 0.18 with a combined significance of 5.9σ when both run 1 and run 2 results are included[75].

The ATLAS result based on 36 fb^{-1} of run 2 data and run 1 results shows a significance[76] of 6.4σ and measures a cross-section in agreement with the 125 GeV Higgs boson prediction. Overall the decay rate for $H \rightarrow \tau^-\tau^+$ was found to be very close to that expected for a Higgs boson with a mass of 125 GeV.

The Higgs boson coupling to the bottom quarks. The bottom quark is the heaviest quark accessible in Higgs boson decays, and has a scheme-dependent mass m_b of 4.2 GeV (REF.[62]). (This is its mass observed at the energy scale m_b quoted with respect to a procedure for calculating radiative corrections called $\overline{MS}$). Free quarks are not observable in nature. Instead, at the LHC, quarks hadronize in jets of particles, resulting from the colour force that connects the produced quarks and breaks up into colourless hadrons, dominantly mesons. Hadrons containing a b-(anti)quark have short lifetimes, typically around 10^{-12} seconds, and thus cross distances in the detector of typically a few millimetres to centimetres, a feature that can be efficiently exploited in experiments to tag particle jets that contain a b-quark. The branching ratio for a 125 GeV Higgs boson into a b plus anti-b quark pair is 58% and constitutes the largest Higgs boson decay channel at this mass value. However, the cross-sections of b plus anti-b quarks produced by SM background processes are seven orders of magnitude larger than the Higgs boson production cross-section, and hence largely dominate the search regions.

Experimentalists have been able to reduce these backgrounds dramatically by selecting special kinematic regions and by using additional event information, such as additional associated jets and, in particular, heavy vector W and Z bosons (where the W and Z bosons decay leptonically), to extract the Higgs boson to bottom quark decay signal. In 2018 both experiments announced the observation of this decay channel. ATLAS reported a $H \rightarrow b\bar{b}$ decay signal with 5.4σ and a signal strength of 1.01 ± 0.20 based on run 2 data of up to 79.8 fb^{-1} and on run 1 data of about 25 fb^{-1} (REF.[77]). CMS observed this channel with 5.6σ significance and a signal strength of 1.04 ± 0.20 based on run 2 data of 41.3 fb^{-1} and on run 1 data of about 25 fb^{-1} (REF.[78]). Hence, the $H \rightarrow b\bar{b}$ decay rate is consistent with the expectations for a 125 GeV Higgs boson. FIGURE 3 shows an event display of a candidate $H \rightarrow b\bar{b}$ decay (FIG. 3a), and the distribution of the m_{bb} invariant mass (FIG. 3b), showing the $Z \rightarrow b\bar{b}$ (grey) and $H \rightarrow b\bar{b}$ (red) signal.

The Higgs boson coupling to muons. With the Higgs boson decay channels to the third-generation fermions (b-quarks and tau leptons) firmly established, the natural next question is: what about the second-generation fermions? Since these particles have lower masses and the signals are often subject to larger backgrounds, extracting information from the data becomes increasingly challenging. However, these measurements are of utmost importance to consolidate the scenario of the long-sought BEH mechanism.

The branching ratio of the $H \rightarrow \mu^-\mu^+$ decay in the SM for a Higgs boson of 125 GeV is small, namely 2.18×10^{-4}, but the final state is very simple: it amounts to a search for two oppositely charged muons which have large transverse momenta, of the order of several tens of gigaelectronvolts (GeVs) in the laboratory frame, and can be efficiently selected and reconstructed by the experiments. The signal resides on a large background tail: the Z boson to muon pair cross-section is five orders of magnitude larger than the expected signal.

The hunt for the $H \rightarrow \mu^-\mu^+$ decays started early on. Any observed signal would have been unexpected at the initial LHC luminosity since for a true Higgs particle this decay is expected to be strongly suppressed compared with, for example, the Higgs boson to $\tau^-\tau^*$ decay, and would have been evidence that the newly found particle was not the SM Higgs boson! Indeed, no evidence for this decay was found in the run 1 data.

The full set of the run 2 data was more recently used by ATLAS and CMS to search for this channel. The large

Tree-level interference
A cross term in squaring the amplitude for Higgs boson production, where the Higgs particle is liberated either from a W boson or from a top quark. This is specified to distinguish the loop level interference that occurs in the diphoton decay channel.

Decay channel
A collision final state involving a specific decay mode of the Higgs boson (for example, two photons, four leptons, two vector bosons, two fermions and so on).

Production channel
A collision final state involving a specific production mode of the Higgs boson (for example, gluon fusion, vector boson fusion, associated production with a vector boson, a pair of top quarks and so on).

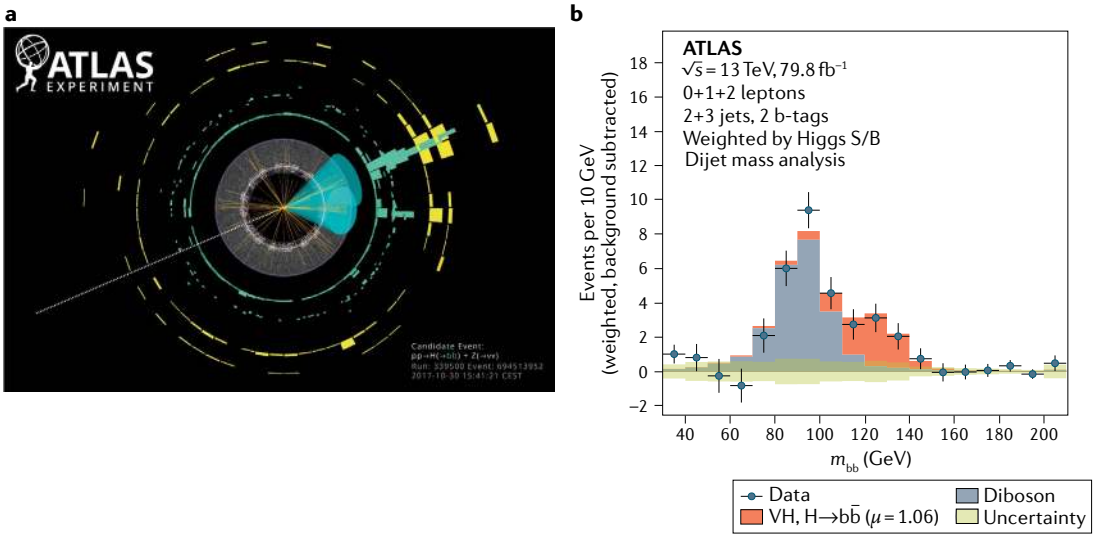

Fig. 3 | **Bottom quark production in Higgs boson decays. a** | An event display of a candidate $H \to b\bar{b}$ decay in the plane transverse to the beam axis; the blue cones illustrate the two reconstructed jets of the b-quark decays. **b** | The distribution of the m_{bb} invariant mass, showing the $Z \to b\bar{b}$ (grey) and $H \to b\bar{b}$ signal (red) signal. Panel **a** photograph: ATLAS Collaboration; copyright: CERN; panel **b** reprinted from REF.[77], CC BY 4.0.

background of mostly Drell–Yan di-muon production required the experiments to use sophisticated tools such as machine learning algorithms to extract a significant signal. In summer 2020, after considerable effort, the experiments were successful and could report the first evidence for $H \to \mu^-\mu^+$ production. CMS reported[79] an observed significance of 3σ and a signal strength of 1.19 ± 0.43. ATLAS reported[80] an observed significance of 2σ and a signal strength of 1.2 ± 0.6.

FIGURE 4 shows an event display of a candidate $H \to \mu^-\mu^+$ decay (FIG. 4a), and the distribution of the $m_{\mu\mu}$ invariant mass (FIG. 4b).

Clearly, these results open up a new research programme for the Higgs boson at the LHC: the detailed study of the second-generation fermion couplings to the Higgs boson. At present, the precision of the results is statistics-limited, a limitation that will be overcome with the advent of the high-luminosity run of the LHC that is expected to start well before the end of the decade.

Similar searches for the decays of the Higgs boson to a pair of electrons have also been carried out by ATLAS[81] and CMS[82], excluding branching fractions of 3.6×10^{-4}. Given the measurement of the branching fraction of Higgs boson decays to tau particles and the evidence for the decay of the Higgs boson to muons, both compatible with the SM expectation, the above limit represents yet another confirmation of the non-universal nature of the Higgs boson Yukawa coupling. Non-flavour diagonal decays of the Higgs boson to an electron and a muon have also been searched for by ATLAS[81].

The Higgs boson couplings to lighter quarks. The quarks of the second-generation fermions have a scheme-dependent mass of 1.27 GeV for the charm quark, c, and a current quark mass of about 90 MeV for the strange quark, s (REF.[62]). The channel $H \to c\bar{c}$ has a branching ratio of 2.8% for a 125 GeV Higgs boson, a much larger background than for the $H \to b\bar{b}$ decay channel and a less efficient charm tagger compared with bottom quarks, and hence is far more challenging to observe.

Direct searches for $H \to c\bar{c}$ have been performed by the experiments, but at present no evidence for this process can be reported; see the ATLAS analysis[83]. The most sensitive result to date is an experimental sensitivity of a factor of 70 (from CMS; see REF.[84]) above the predicted SM values. Additional data, improved charm tagging and reconstruction efficiencies, and a deeper use of machine learning techniques will no doubt push these sensitivities closer to the SM observable limits, but at this point one cannot yet be sure whether this channel will become detectable at the LHC. Other channels are also pursued, such as $H \to J/\Psi\gamma$ and $H \to \Psi(2S)\gamma$ (REFS[85–87]), the associated production of the Higgs boson with a c-quark[88], and the measurement of the charge asymmetry in the associated production mode of a Higgs boson with a vector boson[89].

The hunt for decays of the Higgs boson to lighter quarks is even more challenging and is not expected to yield detectable signals for SM Higgs boson couplings at the LHC, but these decays have nevertheless been searched for in topologies with a vector meson — ρ (REFS[90,91]); ϕ (REFS[90–92]); J/ψ (REF.[86]); and Υ (REF.[86]) — and a Z boson or a photon.

Overall, wherever the LHC currently has sufficient sensitivity, its data dramatically show that the couplings to fermions are in agreement with the expectations of the predictions from the SM BEH mechanism. Although the Higgs boson's couplings to light fermions are experimentally unknown at present, it has already been established that these couplings cannot be the same for all generations (otherwise the light fermions would have been more copiously produced in Higgs boson decays in the experiments).

Drell–Yan di-muon
A process in which a quark from one incoming proton annihilates with an antiquark from the second proton, producing a photon or Z boson that then decays into a $\mu^+\mu^-$ pair.

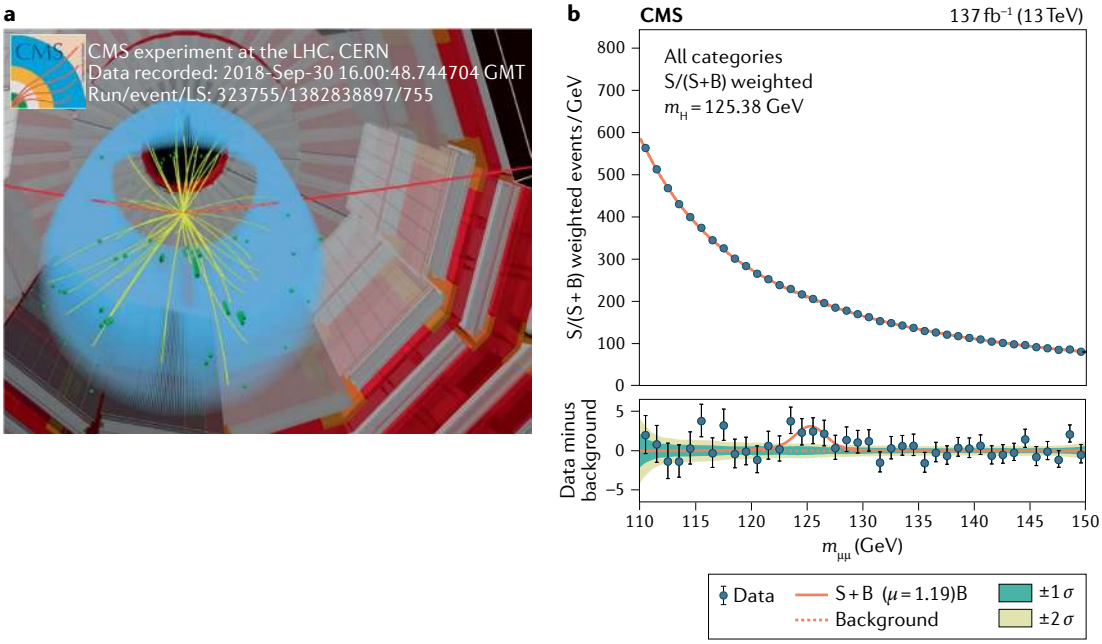

Fig. 4 | **Muon production in Higgs boson decays. a** | A 3D event display of a candidate $H \rightarrow \mu^-\mu^+$ decay illustrating the reconstructed trajectories of the two muons in red; the reconstructed invariant mass of the muon pair is consistent with that of the Higgs boson. **b** | The distribution of the $m_{\mu\mu}$ invariant mass, and data minus background distribution. S denotes the signal, B background and $\mu = 1.19$ is the signal strength. Panel **a** copyright: CERN; panel **b** reprinted from REF.[79], CC BY 4.0.

Summary of measured Higgs properties

In a few years the LHC will conclude its first phase of operation before a major luminosity upgrade, but it is already instructive to outline the picture of this newly found particle that has been emerging so far. The experiments have combined measurements of Higgs boson production cross-sections and branching fractions. These combinations are based on the analyses of the Higgs boson decay modes $H \rightarrow \gamma\gamma$, ZZ, WW, $\tau\tau$, $b\bar{b}$, $\mu\mu$, searches for decays into invisible final states, and on measurements of off-shell Higgs boson production. Such combination studies are made by the experimental collaborations, typically after all individual channels have been analysed for a large fraction of the recorded data. ATLAS (CMS) has produced such a combination based on using up to 79.8 fb^{-1} (35.9 fb^{-1}) of proton–proton collision data[93,94] collected in run 2 and found overall global signal strength of the combined fit of all channels to be $\mu_S = 1.11^{+0.09}_{-0.08}$ ($\mu_S = 1.17 \pm 0.10$), which is close to one, the expected SM value. The final combined run 2 analysis based on 139 fb^{-1} from each experiment is likely to be available towards the end of 2021.

These results are interpreted in terms of so-called coupling modifiers κ applied to the SM couplings of the Higgs boson to other particles. The coupling modifiers are derived from global fits to all the measurements in different production and decay channels assuming SM relations between the channels, and therefore these κ values do not measure the couplings directly, but rather show the levels of deviation from the SM expectations. It is possible to test the coupling-strength scale factors. The results are illustrated for the different decay channels in FIG. 5a and show the consistency of the couplings of the Higgs boson to vector bosons and fermions. An overall fit gives $\kappa_V = 1.05 \pm 0.04$ and $\kappa_F = 1.05 \pm 0.09$, that is, values close to one, the SM prediction. The precision achieved so far in these measurements relies not only on the excellent performance of the machine (accelerator) and the experiments (detectors), but also on the remarkable progress made in the theoretical predictions of the processes at stake, their simulation and their efficient reconstruction.

One of the most prominent achievements to date is the measurement of the hierarchy of the relative coupling strengths of the different particles to the Higgs boson. In the SM, the Yukawa coupling between the Higgs boson and the fermions, y_F, is proportional to the fermion masses m_F, whereas the coupling to weak bosons is proportional to the square of the vector boson masses m_V, with the latter following from the W and Z coupling to the Higgs boson via the SM gauge covariant derivative[5–7]. These relations are confirmed by the data in a dramatic way in FIG. 5b. These are the fruits of the first 10 years of data taking and careful analysis at the LHC.

Another landmark result of the first phase of the LHC is the fact that, so far, no new phenomena beyond those predicted by the SM have been observed. This has led the experimental and the theoretical communities to perform combined interpretations of all measurements in Higgs, electroweak and top physics in a framework where the SM is considered as an effective field theory[55,95–99].

With the full LHC dataset, the precision of the couplings of the Higgs boson is expected to reach between 1% and 2% for the couplings to gauge bosons and between 2% and 4% for couplings to the charged fermions of the third generation. Good precision will also be achieved for the Higgs boson to muons coupling and

Mass shell
Physical particles with the correct energy–momentum relation are called on-shell or on-mass shell; otherwise, they are called off-shell or off-mass shell. Off-shell particles are virtual and can exist in interaction processes.

to Zγ pairs[89]. The final precision for Higgs boson coupling measurements at the LHC in the future will mostly be limited by the precision of theoretical predictions of signal and background processes.

The width of the Higgs particle, which is a measure of its lifetime and is expected to be 4.1 MeV, cannot be extracted from the observed experimental resonance lineshape owing to limited experimental resolution of the detectors. Instead, an indirect method is used, that compares the production rate of the on-mass shell Higgs boson with the production of the Higgs boson far off-mass shell, where it acts as a propagator in the production of a pair of vector bosons (W and Z, both on-mass shell). Although the on-mass shell rate depends on the Higgs boson's width, the off-mass shell rates do not and so comparing the rates of the two regimes gives an estimate of the Higgs boson's natural width. This method assumes that the energy dependence of the Higgs boson couplings do not deviate significantly from those expected from the SM. CMS extracted with 80.2 fb^{-1} of data a central value of the width to be constrained to $3.2\pm^{2.8}_{2.2}$ MeV at 68% CL, and a range constrained to [0.08, 9.16] MeV at 95% CL[100]. The ATLAS experiment reported an upper limit of 14.4 MeV, based on 36 fb^{-1} of data[101]. It is interesting that new results also provide a lower limit of the allowed range width of the Higgs boson, but the measurement is currently still statistics-limited. Since the ultimate LHC data sample will have 20-fold higher statistics, this method is most promising to experimentally verify the Higgs boson's width within the next 15 years. Note, however, that there is a model-dependent assumption underlying this method: that no extra new particles contribute to the off-shell mass rate (that is to the rate or luminosity times cross-section of Higgs particles with mass larger than 180 GeV), which would invalidate this width extraction.

Pinning down the Higgs boson's width provides a probe beyond the SM because it accounts for possible invisible decays into particles that do not interact in the detectors, such as the dark matter candidates discussed in REFS[102,103]. In the SM such decays are expected from neutrinos in the final state (from Z boson decays) and are rare, with a branching fraction of approximately 10^{-3}. Invisible Higgs boson decays can be directly searched for in event topologies with significant missing transverse momentum. Both ATLAS and CMS have performed searches for these decays in all the main production modes, already yielding stringent constraints on the invisible decay width[104] of about 20%. This constraint can be translated into limits on dark matter searches as shown[104,105] in FIG. 6. The comparison is performed in the context of Higgs portal models[106]. The translation of the H → invisible result into a weak interacting massive particle (WIMP)-nucleon scattering cross-section $\sigma_{\text{WIMP-N}}$ relies on an effective field theory approach under the assumption that an invisible Higgs boson decay to a pair of WIMPs is kinematically possible and that the WIMP is a scalar or a fermion[107–109]. The excluded $\sigma_{\text{WIMP-N}}$ values range down to 2×10^{-46} cm^2 in the fermion WIMP scenario, probing a new exclusion region for masses below 10 GeV. When extrapolated to the full LHC dataset, including the high luminosity phase, a projected sensitivity of 2.5% should be reached.

Higgs boson self-coupling

In its SM form of equation (1), the self coupling λ is related to the Higgs boson's mass and VEV, as indicated in equation (3), and induces three Higgs and four Higgs boson interaction vertices after the spontaneous breaking

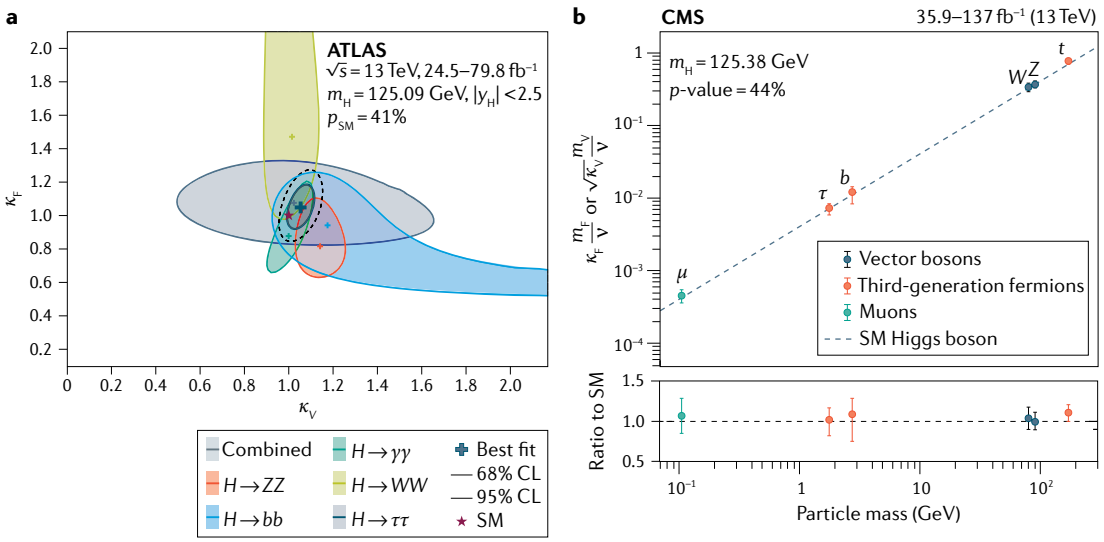

Fig. 5 | **Summary of measured Higgs boson properties. a** | Negative log-likelihood contours at 68% and 95% confidence level (CL) for the SM coupling modifiers in the (κ_V, κ_F) plane for the individual decay modes and their combination, assuming the coupling strengths to fermions and vector bosons to be positive. No contributions from invisible or undetected Higgs boson decays are assumed. The best-fit value for each measurement is indicated by a cross and the standard model (SM) hypothesis is indicated by a star. **b** | The best-fit estimates for the reduced coupling modifiers extracted for fermions and weak bosons from the resolved κ-framework compared with their corresponding prediction from the SM. The error bars represent 68% CL intervals for the measured parameters. In the lower panel, the ratios of the measured coupling modifiers values to their SM predictions are shown. Panel **a** reprinted from REF.[93], CC BY 4.0; panel **b** reprinted from REF.[79], CC BY 4.0.

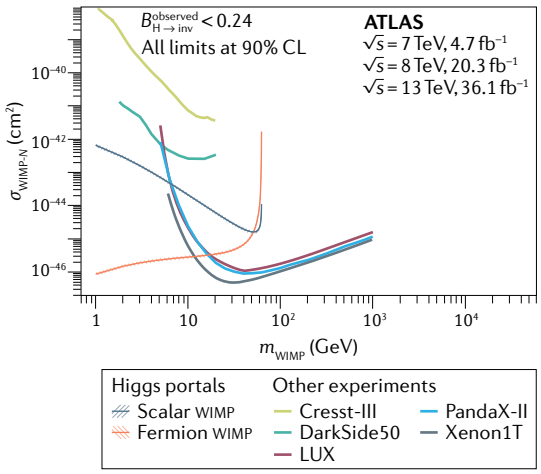

Fig. 6 | **Comparison of the upper limits at 90% CL from direct detection experiments[209–213] on the spin-independent weak interacting massive particle (WIMP)-nucleon scattering cross-section σ_{WIMP-N} with the observed exclusion limits, assuming Higgs portal scenarios where the 125 GeV Higgs boson decays to a pair of dark matter particles[106] with the Higgs boson as the unique link between SM and dark matter particles.** The regions above the limit contours are excluded in the range shown in the plot. m_{WIMP} denotes the WIMP mass; $B^{observed}_{H\to inv} < 0.24$ is the exclusion limit on the invisible Higgs branching ratio from runs 1 and 2 at 90% CL. Figure reprinted from REF.[105], CC BY 4.0.

of the electroweak symmetry. The measurement of the Higgs boson self-interaction is of fundamental importance and the implications of such measurements are discussed in the next section.

With knowledge of the value of the Higgs boson mass, within the SM the self-coupling of the Higgs boson became known through the formula $m_H^2 = 2\lambda v^2$; see equation (3). However, its direct measurement is key[110] to understanding whether the electroweak symmetry breaking occurs as a crossover, as expected in the SM, or as a strong first-order phase transition in the early Universe, which would be crucial to our understanding of baryogenesis and has implications for possible gravitational-wave signals. Higgs self-coupling is one of the deepest questions of the SM and may provide a portal to new physics beyond it. Experimentally, this can be addressed via the measurement of the production of multiple Higgs bosons.

With the run 2 dataset, a major effort to perform complete analyses in a number of final state channels, combining a variety of decay modes for each Higgs boson $\gamma\gamma$, $b\bar{b}$, $\tau^+\tau^-$, WW* seeking the highest sensitivity to the di-Higgs (HH) boson production was made[111,112]. The final state that was immediately recognized as providing an optimal compromise between the number of events produced and a decent signal-to-background ratio, was $(H\to b\bar{b})(H\to\gamma\gamma)$, but adding additional channels can substantially enhance the sensitivity.

The net HH production receives contributions from processes that involve Higgs boson self-interactions and other interactions that are not sensitive to λ. The measurement of the kinematics of the HH system is crucial to disentangling the different contributions and inferring information on λ (REF.[113]). Individual experiment combinations with a partial run 2 dataset show that limits below 10 times the SM expected rate can be set on the HH production cross-section. An analysis with the full run 2 dataset from CMS in the $b\bar{b}\gamma\gamma$ channel enables the exclusion of values of the trilinear coupling smaller than −3.3 and larger than 8.5 times the SM expectation[114]. With the full run 2 dataset, the ATLAS experiment performed a search for the $HH\to b\bar{b}b\bar{b}$ final state in the electroweak vector boson fusion production mode[115]; this process has a cross-section smaller by approximately one order of magnitude, but is sensitive to HHVV (c_{2V}) coupling and has set a limit of $-1.02 < c_{2V} < 2.71$. The sensitivity of these studies is still far from a measurement of the trilinear coupling. However, it suggests that with the full luminosity for the entire LHC programme a combined sensitivity of 4 standard deviations for observing HH production can be obtained[89].

Another possible way to measure the trilinear coupling is to constrain λ indirectly through its loop level effect on single Higgs boson production[116]. However, such constraints are model-dependent and typically rather weak.

Additional Higgs bosons and non-SM interactions

Although present data suggest that the discovered Higgs particle is very SM-like, the experiments have nevertheless tried to expose it as an imposter, by searching for unexpected Higgs boson production processes or unexpected decays — without success so far. Is it possible that there is more than one Higgs or Higgs-like boson lurking in the wealth of data collected at the LHC? Within the SM only one fundamental scalar particle is expected, but in many of the SM extensions the full Higgs family would contain several additional members. Searches for both lighter and more massive (pseudo-)scalar particles, neutral and charged, have been carried out, with no evidence found so far. A recent survey of the searches for additional Higgs bosons is reported in REFS[62,117].

CP violation is an essential ingredient for our understanding of the matter–antimatter asymmetry in the Universe. Within the SM, very precise electric dipole moment measurements, in particular of the electron[11], measured to be $|d_e/e| < 1.1\times10^{-29}$ cm where e is the electric charge of the electron, impose very stringent limits on CP violation in the Higgs Yukawa sector[118]. These constraints are model-dependent, so probing the CP properties of the Higgs boson directly is mandatory. The SM Higgs boson is CP-even. Non-CP-even couplings of the Higgs boson to vector bosons have been searched for in Higgs boson decays to ZZ* and WW*[100,119] and through production in associated channels[120,121], using several decay modes. CP-odd couplings to fermions have been searched for both in the decay of the Higgs boson to a pair of tau leptons[122] and in the $t\bar{t}H$ production mode with the subsequent decay of the Higgs boson to a pair of photons[66,123]. No significant CP-violating effects have been observed.

In the SM, the Yukawa couplings are diagonalized in the mass matrix; there are no off-diagonal terms. There

Trilinear coupling
The interaction vertex involving three Higgs particles (and no others).

are ways to evade this via effective dimension-6 operators yielding models with off-diagonal Yukawa couplings, which are of particular interest because they can break the relation between the masses and the couplings and can generate additional Higgs boson self-coupling terms. These operators describe multi-particle correlations beyond the minimal SM interactions and are suppressed by the square of some large mass scale that represents the scale of new physics. The constraints from light quark or lepton flavour changing neutral currents, such as for instance $\mu \to e\gamma$, are very strong. However, in the case of heavier fermions, for example, from $\tau \to \mu\gamma$ or $\tau \to 3\mu$, these constraints are less stringent and the strongest bound on off-diagonal τ–μ Yukawa couplings now comes from the search for Higgs boson decays to a tau plus muon pair, with bounds on the mixing term $|Y_{\tau\mu}|$ close to 10^{-3} (REFS[124,125]). LHC data so far have revealed no evidence of higher-dimensional operator correlations divided by powers of any large mass scale below the few-TeV range[126,127].

In the quark sector the existence of the Higgs boson at a mass of around 125 GeV has opened up an interesting opportunity to search for flavour-changing neutral current (FCNC) decays of the top quark to a Higgs boson and a charm quark or an up quark. FCNC top quark decays have been searched for in multiple subsequent Higgs boson decay channels, including the diphoton, WW*, $\tau^+\tau^-$ and $b\bar{b}$ (REFS[128–134]). Bounds on top FCNC decay branching fractions down to approximately 0.2% are reached. These channels complement other FCNC top decays searches with a photon or a Z boson in the final state instead of the Higgs boson.

In summary, the Higgs boson's properties measured at the LHC so far are consistent with the SM expectations within the present measurement precision. Furthermore, with a mass of 125 GeV, the effects of the predicted Higgs boson quantum corrections on electroweak observables within the SM are entirely compatible with the precision measurements carried out at the LEP collider at CERN and the Stanford Linear Collider at SLAC, and at low energies[135].

No evidence for additional Higgs bosons, Higgs boson decays into undetected particles, or CP, FCNC or lepton flavour-violating effects in Higgs boson decays have yet been observed. These tremendous successes of the SM should, however, not deter us from searching for answers to fundamental open questions. All these experimental searches will therefore continue with the same vigour within the anticipated, much larger, datasets.

Vacuum stability and hierarchies of scales

If taken to be the SM Higgs boson, the boson discovered at LHC completes the SM. However, it is accompanied by intriguing observations, including possible clues to new physics. Up to what energy might the SM work as the theory of particle interactions, that is, what is the ultraviolet limit of the SM when taken as an effective theory? What new interactions might lie beyond the SM? Important theoretical issues are the stability of the Higgs vacuum and the small size of the electroweak scale and the Higgs boson's mass relative to the Planck scale, 1.2×10^{19} GeV, where quantum gravity effects might apply.

Vacuum stability. With the discovered boson, the SM is perturbative and predictive when extrapolated to very high energies. Interestingly, if the SM is extrapolated with its measured couplings up to the Planck scale and it is assumed that there are no couplings to extra particles or new interactions, then the Higgs vacuum sits very close to the border between stable and metastable[136–143], within 1.3 standard deviations of being stable[143]. In the case of a metastable vacuum, there would be a second minimum in the Higgs potential with a lower value than that measured at our energy scale (as shown in FIG. 1b) after inclusion of radiative corrections. For an unstable vacuum the BEH potential would become unbounded from below at large values of the BEH field.

Vacuum stability depends on the ultraviolet behaviour of the Higgs boson self-coupling λ, that is, its behaviour at the maximum possible energy scales. The SM couplings evolve with changing resolution (energy scale) according to the renormalization group, as shown in FIG. 7a. The weak SU(2) and QCD SU(3) couplings, g and g_s, are asymptotically free, with $\alpha_i = g_i^2/4\pi$ decaying logarithmically with increasing resolution, whereas the U(1) coupling g' is non asymptotically free, rising in the ultraviolet. The top quark Yukawa coupling y_t decays with increasing resolution. The running of the Higgs boson self-coupling λ determines the stability of the electroweak vacuum. Instability sets in if λ crosses zero deep in the ultraviolet part of the spectrum and involves a delicate balance of SM parameters. With the SM parameters measured at the LHC, λ decreases with increasing resolution. This behaviour is dominated by the large Higgs boson coupling to the top quark (and also QCD interactions of the top). Without this coupling, λ would rise in the ultraviolet. In FIG. 7a, λ crosses zero around 10^{10} GeV with the top quark pole mass of $m_t = 173$ GeV and $m_H = 125$ GeV. This situation signals a metastable vacuum with lifetime greater than about 10^{600} years (REF.[137]), much longer than the present age of the Universe, about 13.8 billion years (see also FIG. 1b). FIGURE 7b shows the sensitivity of vacuum stability to small changes in m_t. If the top mass is taken as 171 GeV in these calculations, the vacuum stays stable up to the Planck scale. The measured 125 GeV Higgs boson mass is close to the minimum needed for vacuum stability with the measured top quark mass.

The SM revealed by current experiments — assuming there are no extra particles at higher energies — is strongly correlated with its behaviour in the extreme ultraviolet, which might suggest something deeper about the origin of the SM.

It is important to emphasize the large extrapolations in these calculations when evolving the SM couplings up to the Planck scale. The existence of new physics, even at the largest scales, can affect the vacuum stability[144]. Modulo this caveat, the Higgs vacuum sitting 'close to the edge' of stable and metastable suggests possible new critical phenomena in the deep ultraviolet. One possible way to interpret this situation is a statistical system in the ultraviolet, near to the Planck scale, close to its critical point[136,137,142]. As a general rule, theories with new interactions and new particles at higher energies should make the vacuum more stable rather than less!

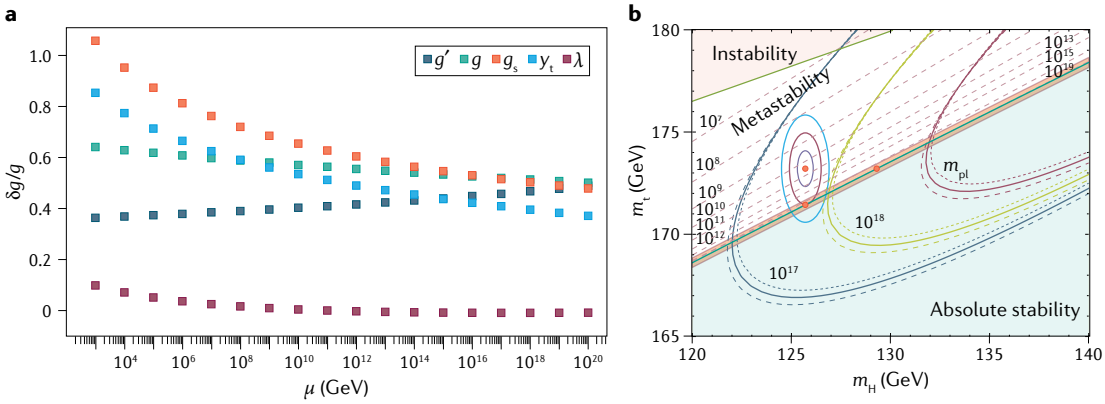

Fig. 7 | **Vacuum stability and ultraviolet behaviour of the SM. a** | Running of the standard model gauge couplings g, g', g_s for the electroweak SU(2) and U(1) and colour SU(3) interactions, the top quark Yukawa coupling y_t and Higgs boson self-coupling λ as a function of the energy scale μ. **b** | Phase diagram of vacuum (meta)stability as a function of the top quark and Higgs boson masses with one-, two- and three-standard-deviation ellipses. The dotted lines refer to the scale where λ touches zero. The parabola-like lines are contours describing the mass parameters, leading to a vanishing rate of change of λ at fixed large scales. Here m_t is the top quark mass, m_H is the Higgs mass and m_{Pl} is the Planck mass. Panel **a** reprinted from REF.[185], CC BY 4.0, with the couplings evaluated using the C++ code in REF.[214]; panel **b** adapted with permission from REF.[143], APS.

Scale hierarchies and the origin of the SM gauge symmetries. The Higgs boson's mass is very much less than the Planck scale despite quantum corrections, which naively act to push its mass towards the deep ultraviolet. Under renormalization, the Higgs boson's mass squared comes with a quadratically divergent counterterm resulting from the Higgs boson self-energy, namely:

$$m^2_{\mathrm{H\ bare}} = m^2_{\mathrm{H\ ren}} + \delta m^2_{\mathrm{H}}, \tag{4}$$

where:

$$\delta m^2_{\mathrm{H}} = \frac{K^2}{16\pi^2}\frac{6}{v^2}(m^2_{\mathrm{H}} + m^2_Z + 2m^2_{\mathrm{W}} - 4m^2_{\mathrm{t}}) \tag{5}$$

relates the renormalized and bare Higgs boson masses, $m_{\mathrm{H\,ren}}$ and $m_{\mathrm{H\ bare}}$ respectively, and small contributions from lighter mass quarks are neglected.

Here K is an ultraviolet cut-off scale on the momentum integrals, characterizing the limit to which the SM should work. The renormalized mass is the mass extracted from experiments. For a textbook discussion of bare and renormalized mass parameters; see REF.[6]. If K is taken as a physical scale, for example, the Planck scale, then why is the physical Higgs boson's mass so small compared with the cut-off? This question, called the hierarchy or naturalness puzzle, has attracted much theoretical attention[145,146].

What physics stabilizes the value of m_H, keeping it so much below the Planck mass? One possibility is that the Higgs boson's mass is fine tuned, perhaps through some kind of environmental selection and perhaps in connection with the vacuum stability of the SM. Alternatively, the SM quantum correction to the Higgs boson's mass, which is dominated by the top quark contribution, might be cancelled by any new particles that couple to the Higgs boson. However, such particles have so far not been seen in the mass range of the LHC. Likewise, any composite structure to the Higgs boson would soften the ultraviolet divergences, but there is no evidence for this in the present data. Searches for extra particles and a possible composite Higgs structure will continue in the coming years with the increased luminosity at the LHC.

The SM is a mathematically consistent theory up to the Planck scale, but is it also physically complete up to the Planck scale? New physics is needed to describe neutrino masses, dark matter and the matter–antimatter asymmetry in the Universe, but the scale where it first appears is an open question. It would be very surprising if there is no new physics below the Planck scale given these phenomena. In the absence of new physics, the naturalness puzzle remains, which has inspired much thinking about possible extra particles. Theoretical attempts to resolve this puzzle include weakly coupled models with a popular candidate being supersymmetry (SUSY)[147], which — if present in Nature — would be a new symmetry between bosons and fermions. Strongly coupled models, where the Higgs boson is considered as a bound state of new dynamics that are strong at the weak scale, are an alternative solution to SUSY. In such scenarios the 'lightness' of the Higgs boson can be explained if the Higgs boson turns out to be a pseudo-Nambu–Goldstone boson. Such models include the so-called little Higgs[148,149], twin Higgs[150] and partial compositeness[151] models. For a comprehensive review of these ideas and their phenomenology see chapter 11 of REF.[62], with possible alternatives to an elementary Higgs boson also discussed in REF.[152].

A related issue is the deeper origin of the gauge symmetries of particle physics. Could the electroweak and QCD interactions unify in the ultraviolet within some larger gauge group? The ultimate dream of this grand unification approach is unification of the SM forces with gravity close to the Planck scale. With unification one expects the running gauge couplings of the SM to meet in the ultraviolet. They do come close (see FIG. 7a), but without exactly crossing. Crossing could be achieved

with the addition of SUSY, at TeV energies[153], a theory that might also provide a dark matter candidate particle. Although the simplest SUSY models would have preferred a Higgs boson mass close to the measured value, the absence of any sign of new SUSY particles in LHC experiments means that these models are now strongly constrained[8,154–156]. The present status of minimal SUSY model predictions for Higgs boson mass(es) is discussed in REF.[157]. Any new symmetries in the ultraviolet must be strongly broken so that they are not seen at the energies of current experiments, meaning that there is a trade-off: the extra symmetry that might exist at higher energies also comes with a (perhaps large) number of new parameters needing extra explanation.

Modulo the large extrapolations involved and any new particles waiting to be discovered at higher energies, it is worth not discarding the idea that the SM might work to very high energies close to the Planck scale. In this alternative scenario, it is plausible that the SM might behave as an emergent effective theory with gauge symmetries 'dissolving' in the extreme ultraviolet[142,158–163]. That is, the SM particles, including the Higgs and gauge bosons, could be the long-range, collective excitations of a statistical system near its critical point that resides close to the Planck scale[142]. Emergent gauge symmetries, where symmetry is created as well as broken, are important in quantum many-body systems, such as high-temperature superconductors[164], in topological phases of matter[165] and in the low-energy limit of the Hubbard model[166] used in quantum simulations of gauge theories[167,168]. Emergent gauge symmetry can arise in association with an infrared fixed point in the renormalization group[169].

Gauge symmetry and renormalizability constrain the global symmetries of the SM at mass dimension four[162]. If the SM is an effective theory emerging in the infrared, low-energy global symmetries such as lepton and baryon-number conservation can be broken through additional (non-renormalizable) higher-dimensional terms, suppressed by powers of a large mass scale M that characterizes the ultraviolet limit of the effective theory[142,162,163,170].

The tiny neutrino masses suggested by the neutrino oscillation data[171] have a simple interpretation in this picture. If neutrinos with zero electric charge are Majorana particles, meaning they are their own antiparticles, then their masses can be linked to lepton number violation and the dimension-five Weinberg operator[172], suppressed by single power of M, involving just the lepton and Higgs fields with $m_\nu \approx \Lambda_{ew}^2/M$ where $\Lambda_{ew} = 246\,\text{GeV}$ is the electroweak scale and $M \approx 10^{15}\,\text{GeV}$. However, if neutrinos are Dirac particles instead, with their tiny masses coming from Yukawa couplings to the Higgs field, one then has to ask why these Yukawa couplings are so much suppressed relative to the charged lepton couplings, with right-handed neutrinos not participating in electroweak interactions.

The Higgs boson and cosmology

The Higgs boson influences many ideas in cosmology, from thinking about the accelerating expansion of the Universe today to processes in the early Universe.

The Higgs potential generates a large vacuum energy contribution to the cosmological constant or vacuum energy density ρ_{vac}, a prime candidate for the dark energy that drives the accelerating expansion of the Universe. From astrophysics experiments, we have[173] $\rho_{vac} = (0.002\,\text{eV})^4$. In the SM, ρ_{vac} receives contributions from the Higgs and QCD condensates, the zero-point energies of quantum field theory and also a gravitational contribution[174]. Electroweak and QCD contributions are characterized by scales of 246 GeV and 200 MeV, so what cancels them to give the net cosmological constant scale of 0.002 eV? This question has attracted considerable theoretical attention and ideas; see REFS[12,37,174–182].

Present measurements are consistent with a time-independent cosmological constant. The next generation of cosmological surveys will look for any time dependence of dark energy, with sensitivity to any variations from a time-independent cosmological constant of 10% or more[183].

An intriguing issue is the similar size of the cosmological constant scale 0.002 eV to what is expected for the value of light neutrino masses[184]. With a finite cosmological constant, there is no solution of Einstein's equations of general relativity with constant Minkowski metric $g_{\mu\nu}$. Global space–time translational invariance of the vacuum is broken by a finite cosmological constant[174]. Motivated by the success of the SM and special relativity in predicting the outcomes of present experiments, one might suppose that the vacuum including condensates with finite VEVs is space–time translational invariant and that flat space-time is consistent at dimension four. Then, if the SM is treated as an effective theory emergent below a large ultraviolet scale M, the global symmetry might be broken through higher-dimensional terms with the electroweak and QCD scales Λ_{ew} and Λ_{qcd} entering the cosmological constant with the scale of the leading term suppressed by Λ_{ew}/M (that is, with vacuum energy density $\rho_{vac} \approx (\Lambda_{ew}^2/M)^4$ with one factor of Λ_{ew}^2/M for each dimension of space–time)[185,186]. How the Higgs potential relates to space–time structure remains an important issue for cosmology.

One of the main ideas for understanding the matter–antimatter asymmetry in the Universe involves a possible first-order phase transition with the Higgs VEV generated in the early Universe[187,188]. Bubbles with Higgs condensates would be created and expand at the speed of light. This scenario also requires new sources of CP violation beyond the usual SM, with new ideas discussed in REF.[189] together with an extended Higgs sector (for example, including an extra singlet scalar) and quantum tunnelling processes in the vacuum called sphalerons that violate baryon number. Evidence for any first-order electroweak phase transition might show up in future gravitational-wave measurements with the Laser Interferometer Space Antenna (LISA) mission of the European Space Agency[190,191] and the proposed AEDGE experiment[192].

Besides the present accelerating expansion, it is believed that the Universe has undergone an initial period of exponential expansion called inflation, with factor at least 10^{26} in the first about 10^{-33} seconds[14]. Inflation is posited to explain the uniformity with small

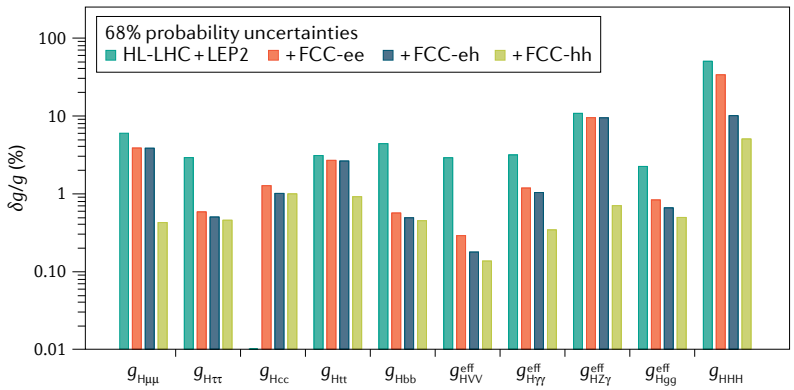

Fig. 8 | **1σ precision reach at the Future Circular Collider (FCC) on the effective Higgs boson couplings to fermions (muons, tau particles, charm quarks, top quarks and b quarks), to vector bosons (W or Z, photons, Zγ and gluons) and the Higgs boson self-coupling in an effective field theory framework.** Absolute precision in the electroweak measurements is assumed. The different bars illustrate the improvements that would be possible by combining each FCC stage with the previous knowledge at that time. The *y*-axis label $\delta g/g$ is the 1σ error on the coupling divided by the coupling value. FCC-ee, FCC electron–positron collider; FCC-eh, FCC electron–proton collider; FCC-hh, FCC hadron collider; HL-LHC, High-Luminosity Large Hadron Collider; LEP2, Large Electron–Positron collider. Figure adapted from REF.[215], CC BY 4.0.

anisotropies in the cosmic microwave background. The particle physics of inflation is unknown, although there are many theoretical ideas, including some where the Higgs boson has an important role[193–195] or where the VEV of a possible time-dependent extra scalar field interpolates between initial inflation and dark energy today[175,177,196,197]. Possible extra fundamental scalars also appear in extended theories of gravitation, beyond minimal general relativity[198]. One theory of inflation connects the Higgs boson to gravitation with non-minimal coupling ξH^2R where R is the Ricci curvature scalar of general relativity and ξ is a dimensionless parameter[193]. The parameters of this model can be chosen to reproduce key features of the cosmic microwave background, the measured scalar spectral index and the tensor-to-scalar ratio.

The Higgs boson may thus play an essential part in the evolution of the Universe from the Big Bang to the physics we see in our experiments today.

Outlook

The Higgs boson discovered at the LHC is the first observed scalar elementary particle, and we are just beginning to understand what this particle can tell us about the Universe.

The precision reached in measuring the Higgs boson properties so far had not been anticipated. Channels thought to be inaccessible have been measured. This extraordinary success is due to several factors: the remarkable operation of the LHC; the robustness of the experiment; the improvements in experimental techniques; the revolution in the theoretical prediction and simulation of the LHC processes; and the 'gift of nature' that the mass of the Higgs boson is precisely at the crossroads of all possible decay modes.

The Higgs boson so far behaves in a very SM-like manner with its couplings to the W and Z gauge bosons, to the third family of charged fermions and to muons from the second family, all consistent with the BEH mechanism of mass generation. But at present it is not known why the particle masses have the values we observe in nature. Furthermore, if the SM is extrapolated up to the Planck scale with the measured Higgs boson and top quark parameters, then the electroweak vacuum sits very close to the border between the stable and metastable regions.

Measurements will be continued, with the LHC run 3 starting in 2022, doubling the collision statistics recorded till now, and later with the high-luminosity upgrade of the LHC[199] expected to start before the end of this decade, for a factor-of-20 increase in the total statistics. These measurements will enable a considerable increase in precision of our knowledge of the Higgs boson's couplings to a precision of a few per cent for many of them. The upgrade will also allow for the first measurements of the Higgs boson's self-interaction, as shown in FIG. 8. Along with increased experimental precision, there is also a need for a more precise theoretical toolbox[54] for optimal extraction of key quantities from the data. Scientists at the LHC secretly hope that the precision measurements will, sooner or later, show deviations from the theoretical predictions, and thus the first cracks in the SM.

The SM is an extraordinary theory, fully consistent up to very high energy scales. We know, however, that it should not be the whole story. To what energy will it continue to hold before new physics emerge? Most likely, the Higgs boson will provide a window to what lies beyond the SM.

Beyond-SM searches include looking for any CP-violating couplings of the Higgs boson, any extended Higgs sector with possible connections to baryogenesis, possible composite structure to the Higgs boson, which could provide indications of unknown underlying dynamics potentially responsible for the BEH mechanism, as well as any decays to possible dark matter candidates that might explain the mysterious 80% missing mass component in the Universe.

The recent European Particle Physics Strategy update[16,17] highlights precision studies of the Higgs boson and its interactions as the main priority for the next high-energy collider. Long-term options past the LHC luminosity upgrade include the Future Circular Collider[200,201] (FCC-ee) or the Compact Linear Collider (CLIC)[202,203] being considered in the context of the future of CERN, with additional electron–positron (e^+e^-) collider options being discussed such as the International Linear Collider (ILC) in Japan[204] and the Circular Electron Positron Collider (CEPC) in China[205]. The circular collider projects also include a proton–proton (FCC-hh) and proton–lepton (FCC-eh) option, typically planned as a next stage following the e^+e^- option. A detailed discussion of the precision that can be reached on Higgs boson property measurements with these different options is reported in REF.[56], with an example for the FCC facility shown in FIG. 8.

Electron–positron colliders cannot reach centre-of-mass energies as high as those of proton–proton

colliders, but benefit from a much cleaner initial collision state, consisting of fundamental particles with well-defined energies entering the interactions. In particular, at electron–positron colliders, Higgs production could be measured inclusively from its presence as a recoil to the Z in $e^+e^- \rightarrow$ HZ events, allowing the absolute measurement of the Higgs boson's coupling to the Z boson.

As shown in FIG. 8, sub-per-cent precision on the couplings of the Higgs boson to other gauge bosons and charged fermions of second and third generation (except the strange quark) can be achieved in e^+e^- collisions where the precision coupling of the Higgs boson to gauge bosons will reach the per mille level, the couplings to bottom quarks, tau particles and muons will reach the level of 4 per mille and the coupling to charm quarks will reach the per cent level[56]. In addition, the prospect of measuring, or at least strongly constraining, the couplings to the three lightest quarks and to the electron by dedicated FCC e^+e^- runs at the Higgs boson's mass is being evaluated.

The direct measurement of the Yukawa coupling to top quarks requires high-energy proton–proton collisions, or even higher centre-of-mass energies for e^+e^-, and should reach precision at the per cent level. The study of invisible Higgs boson decays will achieve sensitivities well below the per cent level and thus reach the level of the expected SM rate, driven by Higgs bosons decaying into a pair of Z bosons, which each decay into neutrinos.

To improve significantly on the precision of Higgs boson self-coupling from direct measurements will require high-energy hadron beams, in lepton–hadron or hadron–hadron mode operation, with the highest expected precision of approximately 5% being obtained at a very-high-energy proton–proton collider with centre-of-mass energy of 100 TeV (REF.[56]).

Besides the charged leptons and quarks, the Higgs boson might also play a key part in the generation of neutrino masses, where — if neutrinos are their own antiparticles — the neutrino mass enters through the dimension-five Weinberg operator. Neutrinoless double-β decay experiments aim to look for Majorana neutrinos with the next-generation experiments sensitive to the theoretically interesting mass range[206,207]. The role of the Higgs potential in the vacuum energy density of the Universe is important to our understanding of the origin of dark energy. Signals of possible phase transitions in the early Universe, such as those responsible for baryogenesis, might be spotted in future gravitational-wave measurements.

This rich programme of experiment and theory promises to provide exciting insights into the Higgs boson and its vital role in the physics of the Universe.

Published online 15 July 2021

1. Aad, G. et al. Observation of a new particle in the search for the standard model Higgs boson with the ATLAS detector at the LHC. *Phys. Lett. B* **716**, 1–29 (2012).
2. Chatrchyan, S. et al. Observation of a new boson at a mass of 125 GeV with the CMS experiment at the LHC. *Phys. Lett. B* **716**, 30–61 (2012).
3. Englert, F. Nobel lecture: the BEH mechanism and its scalar boson. *Rev. Mod. Phys.* **86**, 843 (2014).
4. Higgs, P. W. Nobel lecture: evading the Goldstone theorem. *Rev. Mod. Phys.* **86**, 851 (2014).
5. Altarelli, G. Collider physics within the standard model: a primer. Preprint at https://arxiv.org/abs/1303.2842 (2013).
6. Pokorski, S. *Gauge Field Theories* 2nd edn (Cambridge Univ. Press, 2000).
7. Aitchison, I. & Hey, A. *Gauge Theories In Particle Physics: A Practical Introduction* Vol. 2 *Non-Abelian Gauge Theories: QCD and the Electroweak Theory* (CRC Press, 2012).
8. Altarelli, G. The Higgs: so simple yet so unnatural. *Phys. Scr. T* **158**, 014011 (2013).
9. Hanneke, D., Fogwell, S. & Gabrielse, G. New measurement of the electron magnetic moment and the fine structure constant. *Phys. Rev. Lett.* **100**, 120801 (2008).
10. Parker, R. H., Yu, C., Zhong, W., Estey, B. & Müller, H. Measurement of the fine-structure constant as a test of the standard model. *Science* **360**, 191–195 (2018).
11. Andreev, V. et al. Improved limit on the electric dipole moment of the electron. *Nature* **562**, 355–360 (2018).
12. Frieman, J., Turner, M. & Huterer, D. Dark energy and the accelerating universe. *Annu. Rev. Astron. Astrophys.* **46**, 385–432 (2008).
13. Dine, M. & Kusenko, A. The origin of the matter–antimatter asymmetry. *Rev. Mod. Phys.* **76**, 1 (2003).
14. Baumann, D. & Peiris, H. V. Cosmological inflation: theory and observations. *Adv. Sci. Lett.* **2**, 105–120 (2009).
15. Baudis, L. The search for dark matter. *Eur. Rev.* **26**, 70–81 (2018).
16. Gianotti, F. & Giudice, G. A roadmap for the future. *Nat. Phys.* **16**, 997–998 (2020).
17. European Strategy Group. 2020 Update of the European Strategy for Particle Physics. *CERN* https://cds.cern.ch/record/2721370/files/CERN-ESU-015-2020%20Update%20European%20Strategy.pdf (2020).
18. Higgs, P. W. Broken symmetries, massless particles and gauge fields. *Phys. Lett.* **12**, 132–133 (1964).
19. Higgs, P. W. Broken symmetries and the masses of gauge bosons. *Phys. Rev. Lett.* **13**, 508–509 (1964).
20. Higgs, P. W. Spontaneous symmetry breakdown without massless bosons. *Phys. Rev.* **145**, 1156–1163 (1966).
21. Englert, F. & Brout, R. Broken symmetry and the mass of gauge vector mesons. *Phys. Rev. Lett.* **13**, 321–323 (1964).
22. Guralnik, G., Hagen, C. & Kibble, T. Global conservation laws and massless particles. *Phys. Rev. Lett.* **13**, 585–587 (1964).
23. Kibble, T. Symmetry breaking in nonAbelian gauge theories. *Phys. Rev.* **155**, 1554–1561 (1967).
24. Llewellyn Smith, C. High-energy behavior and gauge symmetry. *Phys. Lett. B* **46**, 233–236 (1973).
25. Bell, J. High-energy behavior of tree diagrams in gauge theories. *Nucl. Phys. B* **60**, 427–436 (1973).
26. Cornwall, J. M., Levin, D. N. & Tiktopoulos, G. Uniqueness of spontaneously broken gauge theories. *Phys. Rev. Lett.* **30**, 1268–1270 (1973).
27. Cornwall, J. M., Levin, D. N. & Tiktopoulos, G. Derivation of gauge invariance from high-energy unitarity bounds on the S matrix. *Phys. Rev. D* **10**, 1145 (1974).
28. 't Hooft, G. Renormalizable Lagrangians for massive Yang–Mills fields. *Nucl. Phys. B* **35**, 167–188 (1971).
29. 't Hooft, G. & Veltman, M. J. G. Regularization and renormalization of gauge fields. *Nucl. Phys. B* **44**, 189–213 (1972).
30. Veltman, M. J. G. Perturbation theory of massive Yang–Mills fields. *Nucl. Phys. B* **7**, 637–650 (1968).
31. Anderson, P. W. Plasmons, gauge invariance, and mass. *Phys. Rev.* **130**, 439–442 (1963).
32. Glashow, S. L. Partial symmetries of weak interactions. *Nucl. Phys.* **22**, 579–588 (1961).
33. Weinberg, S. A model of leptons. *Phys. Rev. Lett.* **19**, 1264–1266 (1967).
34. Salam, A. Weak and electromagnetic interactions. In *Proc. 8th Nobel Symp.* C680519, 367–377 (1968).
35. 't Hooft, G. & Veltman, M. J. G. Regularization and renormalization of gauge fields. *Nucl. Phys. B* **44**, 189–213 (1972).
36. Lykken, J. & Spiropulu, M. The future of the Higgs boson. *Phys. Today* **66**, 28–33 (2013).
37. Veltman, M. J. G. Reflections on the Higgs system. CERN-YELLOW-97-05 *CERN* https://cds.cern.ch/record/2654857?ln=en (1997).
38. Carr, B. J. & Rees, M. The anthropic principle and the structure of the physical world. *Nature* **278**, 605–612 (1979).
39. Chanowitz, M. S. The No-Higgs signal: strong WW scattering at the LHC. *Czech. J. Phys.* **55**, B45–B58 (2005).
40. Littlewood, P. B. & Varma, C. M. Amplitude collective modes in superconductors and their coupling to charge-density waves. *Phys. Rev. B* **26**, 4883–4893 (1982).
41. Sherman, D., Pracht, U. S. & Gorshunov, B. et al. The Higgs mode in disordered superconductors close to a quantum phase transition. *Nat. Phys.* **11**, 188–197 (2015).
42. Anderson, P. W. Higgs, Anderson and all that. *Nat. Phys.* **11**, 93 (2015).
43. Shimano, R. & Tsuji, N. Higgs mode in superconductors. *Annu. Rev. Condens. Matter Phys.* **11**, 103–124 (2020).
44. Pekker, D. & Varma, C. Amplitude/Higgs modes in condensed matter physics. *Annu. Rev. Condens. Matter Phys.* **6**, 269–297 (2015).
45. Bruning, O. S. et al. LHC Design Report Vol.1: the LHC Main Ring. *CERN* https://inspirehep.net/literature/656250 (2004).
46. Aad, G. et al. The ATLAS experiment at the CERN Large Hadron Collider. *J. Instrum.* **3**, S08003 (2008).
47. Chatrchyan, S. et al. The CMS experiment at the CERN LHC. *J. Instrum.* **3**, S08004 (2008).
48. Landau, L. On the angular momentum of a system of two photons. *Dokl. Akad. Nauk SSSR* **60**, 207–209 (1948).
49. Yang, C.-N. Selection rules for the dematerialization of a particle into two photons. *Phys. Rev.* **77**, 242–245 (1950).
50. Chatrchyan, S. et al. Study of the mass and spin-parity of the Higgs boson candidate via its decays to Z boson pairs. *Phys. Rev. Lett.* **110**, 081803 (2013).
51. Khachatryan, V. et al. Constraints on the spin-parity and anomalous HVV couplings of the Higgs boson in proton collisions at 7 and 8 TeV. *Phys. Rev. D* **92**, 012004 (2015).
52. Aad, G. et al. Evidence for the spin-0 nature of the Higgs boson using ATLAS data. *Phys. Lett. B* **726**, 120–144 (2013).

53. Dawson, S., Englert, C. & Plehn, T. Higgs physics: it ain't over till it's over. *Phys. Rep.* **816**, 1–85 (2019).
54. Heinrich, G. Collider physics at the precision frontier. *Phys. Rep.* **922**, 1–69 (2021).
55. de Florian, D. et al. Handbook of LHC Higgs cross sections: 4. Deciphering the nature of the Higgs sector. Preprint at https://arxiv.org/abs/1610.07922 (2016).
56. de Blas, J. et al. Higgs Boson studies at future particle colliders. *J. High Energy Phys.* **2020** (01), 139 (2020).
57. Alcaraz, J. et al. A combination of preliminary electroweak measurements and constraints on the standard model. Preprint at https://arxiv.org/abs/hep-ex/0612034 (2006).
58. Aad, G. et al. Combined measurement of the Higgs boson mass in *pp* collisions at $\sqrt{s}=7$ and 8 TeV with the ATLAS and CMS experiments. *Phys. Rev. Lett.* **114**, 191803 (2015).
59. Sirunyan, A. M. et al. A measurement of the Higgs boson mass in the diphoton decay channel. *Phys. Lett. B* **805**, 135425 (2020).
60. Aaboud, M. et al. Measurement of the Higgs boson mass in the $H\rightarrow ZZ^{*}\rightarrow 4\ell$ and $H\rightarrow\gamma\gamma$ channels with $\sqrt{s}=13$ TeV *pp* collisions using the ATLAS detector. *Phys. Lett. B* **784**, 345–366 (2018).
61. d'Enterria, D. On the (Gaussian) maximum at a mass m_H ~ 125 GeV of the product of decay probabilities of the standard model Higgs boson. Preprint at https://arxiv.org/abs/1208.1993 (2012).
62. Zyla, P. et al. (Particle Data Group). Review of Particle Physics. *Prog. Theor. Exp. Phys.* **2020**, 083C01 (2020).
63. Aaboud, M. et al. Observation of Higgs boson production in association with a top quark pair at the LHC with the ATLAS detector. *Phys. Lett. B* **784**, 173–191 (2018).
64. Sirunyan, A. M. et al. Observation of $t\bar{t}H$ production. *Phys. Rev. Lett.* **120**, 231801 (2018).
65. Sirunyan, A. M. et al. Measurements of $t\bar{t}H$ production and the CP structure of the Yukawa interaction between the Higgs boson and top quark in the diphoton decay channel. *Phys. Rev. Lett.* **125**, 061801 (2020).
66. Aad, G. et al. *CP* properties of Higgs boson interactions with top quarks in the $t\bar{t}H$ and *tH* processes using $H\rightarrow\gamma\gamma$ with the ATLAS detector. *Phys. Rev. Lett.* **125**, 061802 (2020).
67. Barger, V., Hagiwara, K. & Zheng, Y.-J. Probing the Higgs Yukawa coupling to the top quark at the LHC via single top+Higgs production. *Phys. Rev. D* **99**, 031701 (2019).
68. Farina, M., Grojean, C., Maltoni, F., Salvioni, E. & Thamm, A. Lifting degeneracies in Higgs couplings using single top production in association with a Higgs boson. *J. High Energy Phys.* **2013** (05), 022 (2013).
69. Sirunyan, A. M. et al. Search for associated production of a Higgs boson and a single top quark in proton-proton collisions at $\sqrt{s}=13$ TeV. *Phys. Rev. D* **99**, 092005 (2019).
70. Sirunyan, A. M. et al. Measurement of the Higgs boson production rate in association with top quarks in final states with electrons, muons, and hadronically decaying tau leptons at $\sqrt{s}=13$ TeV. *Eur. Phys. J. C* **81**, 378 (2021).
71. Chatrchyan, S. et al. Evidence for the 125 GeV Higgs boson decaying to a pair of τ leptons. *J. High Energy Phys.* **2014** (05), 104 (2014).
72. Aad, G. et al. Evidence for the Higgs-boson Yukawa coupling to tau leptons with the ATLAS detector. *J. High Energy Phys.* **2015** (04), 117 (2015).
73. Aad, G. et al. Measurements of the Higgs boson production and decay rates and constraints on its couplings from a combined ATLAS and CMS analysis of the LHC pp collision data at $\sqrt{s}=7$ and 8 TeV. *J. High Energy Phys.* **2016** (08), 045 (2016).
74. Sirunyan, A. M. et al. Search for the associated production of the Higgs boson and a vector boson in proton-proton collisions at $\sqrt{s}=13$ TeV via Higgs boson decays to τ leptons. *J. High Energy Phys.* **2019** (06), 093 (2019).
75. Sirunyan, A. M. et al. Observation of the Higgs boson decay to a pair of τ leptons with the CMS detector. *Phys. Lett. B* **779**, 283–316 (2018).
76. Aaboud, M. et al. Cross-section measurements of the Higgs boson decaying into a pair of τ-leptons in proton-proton collisions at $\sqrt{s}=13$ TeV with the ATLAS detector. *Phys. Rev. D* **99**, 072001 (2019).
77. Aaboud, M. et al. Observation of $H\rightarrow b\bar{b}$ decays and *VH* production with the ATLAS detector. *Phys. Lett. B* **786**, 59–86 (2018).
78. Sirunyan, A. M. et al. Observation of Higgs boson decay to bottom quarks. *Phys. Rev. Lett.* **121**, 121801 (2018).
79. Sirunyan, A. M. et al. Evidence for Higgs boson decay to a pair of muons. *J. High Energy Phys.* **2021** (01), 148 (2021).
80. Aad, G. et al. A search for the dimuon decay of the standard model Higgs boson with the ATLAS detector. *Phys. Lett. B* **812**, 135980 (2021).
81. Aad, G. et al. Search for the Higgs boson decays $H\rightarrow ee$ and $H\rightarrow e\mu$ in *pp* collisions at $\sqrt{s}=13$ TeV with the ATLAS detector. *Phys. Lett. B* **801**, 135148 (2020).
82. Khachatryan, V. et al. Search for a standard model-like Higgs boson in the $\mu^{+}\mu^{-}$ and $e^{+}e^{-}$ decay channels at the LHC. *Phys. Lett. B* **744**, 184–207 (2015).
83. Aaboud, M. et al. Search for the decay of the Higgs boson to charm quarks with the ATLAS experiment. *Phys. Rev. Lett.* **120**, 211802 (2018).
84. Sirunyan, A. M. et al. A search for the standard model Higgs boson decaying to charm quarks. *J. High Energy Phys.* **2020** (03), 131 (2020).
85. Aaboud, M. et al. Searches for exclusive Higgs and *Z* boson decays into $J/\psi\gamma$, $\psi(2S)\gamma$, and $\Upsilon(nS)\gamma$ at $\sqrt{s}=13$ TeV with the ATLAS detector. *Phys. Lett. B* **786**, 134–155 (2018).
86. Aad, G. et al. Search for Higgs and Z boson decays to $J/\psi\gamma$ and $\Upsilon(nS)\gamma$ with the ATLAS detector. *Phys. Rev. Lett.* **114**, 121801 (2015).
87. Sirunyan, A. M. et al. Search for rare decays of Z and Higgs bosons to J/ψ and a photon in proton–proton collisions at $\sqrt{s}=13$ TeV. *Eur. Phys. J. C* **79**, 94 (2019).
88. Brivio, I., Goertz, F. & Isidori, G. Probing the charm quark Yukawa coupling in Higgs + charm production. *Phys. Rev. Lett.* **115**, 211801 (2015).
89. Cepeda, M. et al. Report from Working Group 2: Higgs physics at the HL-LHC and HE-LHC. *CERN Yellow Rep. Monogr.* **7**, 221–584 (2019).
90. Aaboud, M. et al. Search for exclusive Higgs and *Z* boson decays to $\phi\gamma$ and $\rho\gamma$ with the ATLAS detector. *J. High Energy Phys.* **2018** (07), 127 (2018).
91. Sirunyan, A. M. et al. Search for decays of the 125 GeV Higgs boson into a Z boson and a ρ or ϕ meson. *J. High Energy Phys.* **2020** (11), 039 (2020).
92. Aaboud, M. et al. Search for Higgs and *Z* boson decays to $\phi\gamma$ with the ATLAS detector. *Phys. Rev. Lett.* **117**, 111802 (2016).
93. Aad, G. et al. Combined measurements of Higgs boson production and decay using up to 80 fb^{-1} of proton-proton collision data at $\sqrt{s}=13$ TeV collected with the ATLAS experiment. *Phys. Rev. D* **101**, 012002 (2020).
94. Sirunyan, A. M. et al. Combined measurements of Higgs boson couplings in proton–proton collisions at $\sqrt{s}=13$ TeV. *Eur. Phys. J. C* **79**, 421 (2019).
95. Giudice, G., Grojean, C., Pomarol, A. & Rattazzi, R. The strongly-interacting light Higgs. *J. High Energy Phys.* **2007** (06), 045 (2007).
96. Grzadkowski, B., Iskrzynski, M., Misiak, M. & Rosiek, J. Dimension-six terms in the standard model Lagrangian. *J. High Energy Phys.* **2010** (10), 085 (2010).
97. Ellis, J., Sanz, V. & You, T. Complete Higgs sector constraints on dimension-6 operators. *J. High Energy Phys.* **2014** (07), 036 (2014).
98. Falkowski, A. & Riva, F. Model-independent precision constraints on dimension-6 operators. *J. High Energy Phys.* **2015** (02), 039 (2015).
99. Dawson, S., Homiller, S. & Lane, S. D. Putting standard model EFT fits to work. *Phys. Rev. D* **102**, 055012 (2020).
100. Sirunyan, A. M. et al. Measurements of the Higgs boson width and anomalous *HVV* couplings from on-shell and off-shell production in the four-lepton final state. *Phys. Rev. D* **99**, 112003 (2019).
101. Aaboud, M. et al. Constraints on off-shell Higgs boson production and the Higgs boson total width in $ZZ\rightarrow 4\ell$ and $ZZ\rightarrow 2\ell 2\nu$ final states with the ATLAS detector. *Phys. Lett. B* **786**, 223–244 (2018).
102. Arcadi, G., Djouadi, A. & Raidal, M. Dark matter through the Higgs portal. *Phys. Rep.* **842**, 1–180 (2020).
103. Carmona, A., Castellano Ruiz, J. & Neubert, M. A warped scalar portal to fermionic dark matter. *Eur. Phys. J. C* **81**, 58 (2021).
104. Sirunyan, A. M. et al. Search for invisible decays of a Higgs boson produced through vector boson fusion in proton–proton collisions at $\sqrt{s}=13$ TeV. *Phys. Lett. B* **793**, 520–551 (2019).
105. Aaboud, M. et al. Combination of searches for invisible Higgs boson decays with the ATLAS experiment. *Phys. Rev. Lett.* **122**, 231801 (2019).
106. Patt, B. & Wilczek, F. Higgs-field portal into hidden sectors. Preprint at https://arxiv.org/abs/hep-ph/0605188 (2006).
107. Eboli, O. J. & Zeppenfeld, D. Observing an invisible Higgs boson. *Phys. Lett. B* **495**, 147–154 (2000).
108. Fox, P. J., Harnik, R., Kopp, J. & Tsai, Y. Missing energy signatures of dark matter at the LHC. *Phys. Rev. D* **85**, 056011 (2012).
109. De Simone, A., Giudice, G. F. & Strumia, A. Benchmarks for dark matter searches at the LHC. *J. High Energy Phys.* **2014** (06), 081 (2014).
110. Carena, M., Liu, Z. & Riembau, M. Probing the electroweak phase transition via enhanced di-Higgs boson production. *Phys. Rev. D* **97**, 095032 (2018).
111. Aad, G. et al. Combination of searches for Higgs boson pairs in *pp* collisions at $\sqrt{s}=13$ TeV with the ATLAS detector. *Phys. Lett. B* **800**, 135103 (2020).
112. Sirunyan, A. M. et al. Combination of searches for Higgs boson pair production in proton-proton collisions at $\sqrt{s}=13$ TeV. *Phys. Rev. Lett.* **122**, 121803 (2019).
113. Alison, J. et al. Higgs boson potential at colliders: status and perspectives. *Rev. Phys.* **5**, 100045 (2020).
114. Sirunyan, A. M. et al. Search for nonresonant Higgs boson pair production in final states with two bottom quarks and two photons in proton-proton collisions at $\sqrt{s}=13$ TeV. *J. High Energy Phys.* **2021** (03), 257 (2021).
115. Aad, G. et al. Search for the $HH\rightarrow b\bar{b}b\bar{b}$ process via vector-boson fusion production using proton-proton collisions at $HH\rightarrow b\bar{b}b\bar{b}$ TeV with the ATLAS detector. *J. High Energy Phys.* **2020** (07), 108 (2020).
116. Di Vita, S., Grojean, C., Panico, G., Riembau, M. & Vantalon, T. A global view on the Higgs self-coupling. *J. High Energy Phys.* **2017** (09), 069 (2017).
117. Steggemann, J. Extended scalar sectors. *Annu. Rev. Nucl. Part. Sci.* **70**, 197–223 (2020).
118. Brod, J., Haisch, U. & Zupan, J. Constraints on CP-violating Higgs couplings to the third generation. *J. High Energy Phys.* **2013** (11), 180 (2013).
119. Aaboud, M. et al. Measurement of the Higgs boson coupling properties in the $H\rightarrow ZZ^{*}\rightarrow 4\ell$ decay channel at $\sqrt{s}=13$ TeV with the ATLAS detector. *J. High Energy Phys.* **2018** (03), 095 (2018).
120. Aad, G. et al. Test of CP invariance in vector-boson fusion production of the Higgs boson using the optimal observable method in the ditau decay channel with the ATLAS detector. *Eur. Phys. J. C* **76**, 658 (2016).
121. Sirunyan, A. M. et al. Constraints on anomalous *HVV* couplings from the production of Higgs bosons decaying to τ lepton pairs. *Phys. Rev. D* **100**, 112002 (2019).
122. Berge, S., Bernreuther, W., Niepelt, B. & Spiesberger, H. How to pin down the CP quantum numbers of a Higgs boson in its tau decays at the LHC. *Phys. Rev. D* **84**, 116003 (2011).
123. Sirunyan, A. M. et al. Search for production of four top quarks in final states with same-sign or multiple leptons in proton-proton collisions at $\sqrt{s}=13$ TeV. *Eur. Phys. J. C* **80**, 75 (2020).
124. Aad, G. et al. Searches for lepton-flavour-violating decays of the Higgs boson in $\sqrt{s}=13$ TeV pp collisions with the ATLAS detector. *Phys. Lett. B* **800**, 135069 (2020).
125. Sirunyan, A. M. et al. Search for lepton flavour violating decays of the Higgs boson to $\mu\tau$ and $e\tau$ in proton-proton collisions at $\sqrt{s}=13$ TeV. *J. High Energy Phys.* **2018** (06), 001 (2018).
126. Slade, E. Towards global fits in EFT's and new physics implications. *Proc. Sci.* **LHCP2019**, 150 (2019).
127. Ellis, J., Madigan, M., Mimasu, K., Sanz, V. & You, T. Top, Higgs, diboson and electroweak fit to the standard model effective field theory. *J. High Energy Phys.* **2021** (04), 279 (2021).
128. ATLAS Collaboration. Search for top quark decays $t\rightarrow qH$ with $H\rightarrow\gamma\gamma$ using the ATLAS detector. *J. High Energy Phys.* **2014** (06), 008 (2014).
129. ATLAS Collaboration. Search for flavour-changing neutral current top quark decays $t\rightarrow Hq$ in *pp* collisions at $\sqrt{s}=8$ TeV with the ATLAS detector. *J. High Energy Phys.* **2012** (12), 061 (2015).
130. ATLAS Collaboration. Search for top quark decays $t\rightarrow qH$, with $H\rightarrow\gamma\gamma$, in $\sqrt{s}=13$ TeV *pp* collisions using the ATLAS detector. *J. High Energy Phys.* **2017** (10), 129 (2017).
131. ATLAS Collaboration. Search for flavor-changing neutral currents in top quark decays $t\rightarrow Hc$ and $t\rightarrow Hu$ in multilepton final states in proton–proton collisions at $\sqrt{s}=13$ TeV with the ATLAS detector. *Phys. Rev. D* **98**, 032002 (2018).

132. ATLAS Collaboration. Search for top-quark decays $t \to Hq$ with 36 fb^{-1} of pp collision data at $\sqrt{s} = 13$ TeV with the ATLAS detector. *J. High Energy Phys.* **2019** (05), 123 (2019).
133. CMS Collaboration. Search for top quark decays via Higgs-boson-mediated flavor-changing neutral currents in pp collisions at $\sqrt{s} = 8$ TeV. *J. High Energy Phys.* **2017** (02), 079 (2017).
134. CMS Collaboration. Search for the flavor-changing neutral current interactions of the top quark and the Higgs boson which decays into a pair of b quarks at $\sqrt{s} = 13$ TeV. *J. High Energy Phys.* **2018** (06), 102 (2018).
135. Baak, M. Review of electroweak fits of the SM and beyond, after the Higgs discovery — with Gfitter. *Proc. Sci.* **EPS-HEP2013**, 203 (2013).
136. Degrassi, G. et al. Higgs mass and vacuum stability in the standard model at NNLO. *J. High Energy Phys.* **2012** (08), 098 (2012).
137. Buttazzo, D. et al. Investigating the near-criticality of the Higgs boson. *J. High Energy Phys.* **2013** (12), 089 (2013).
138. Bezrukov, F., Kalmykov, M. Y., Kniehl, B. A. & Shaposhnikov, M. Higgs boson mass and new physics. *J. High Energy Phys.* **2012** (10), 140 (2012).
139. Alekhin, S., Djouadi, A. & Moch, S. The top quark and Higgs boson masses and the stability of the electroweak vacuum. *Phys. Lett. B* **716**, 214–219 (2012).
140. Masina, I. Higgs boson and top quark masses as tests of electroweak vacuum stability. *Phys. Rev. D* **87**, 053001 (2013).
141. Hamada, Y., Kawai, H. & Oda, K.-y Bare Higgs mass at Planck scale. *Phys. Rev. D* **87**, 053009 (2013).
142. Jegerlehner, F. The standard model as a low-energy effective theory: what is triggering the Higgs mechanism? *Acta Phys. Polon. B* **45**, 1167 (2014).
143. Bednyakov, A., Kniehl, B., Pikelner, A. & Veretin, O. Stability of the electroweak vacuum: gauge independence and advanced precision. *Phys. Rev. Lett.* **115**, 201802 (2015).
144. Branchina, V. & Messina, E. Stability, Higgs boson mass and new physics. *Phys. Rev. Lett.* **111**, 241801 (2013).
145. Giudice, G. F. Naturally speaking: the naturalness criterion and physics at the LHC. Preprint at https://arxiv.org/abs/0801.2562 (2008).
146. Wells, J. D. Lectures on Higgs boson physics in the standard model and beyond. Preprint at https://arxiv.org/abs/0909.4541 (2009).
147. Wess, J. & Zumino, B. A Lagrangian model invariant under supergauge transformations. *Phys. Lett. B* **49**, 52–54 (1974).
148. Arkani-Hamed, N., Cohen, A. G. & Georgi, H. Electroweak symmetry breaking from dimensional deconstruction. *Phys. Lett. B* **513**, 232–240 (2001).
149. Arkani-Hamed, N., Cohen, A. G., Katz, E. & Nelson, A. E. The littlest Higgs. *J. High Energy Phys.* **2002** (07), 034 (2002).
150. Chacko, Z., Goh, H.-S. & Harnik, R. The twin Higgs: natural electroweak breaking from mirror symmetry. *Phys. Rev. Lett.* **96**, 231802 (2006).
151. Kaplan, D. B. Flavor at SSC energies: a new mechanism for dynamically generated fermion masses. *Nucl. Phys. B* **365**, 259–278 (1991).
152. Csaki, C., Grojean, C. & Terning, J. Alternatives to an elementary Higgs. *Rev. Mod. Phys.* **88**, 045001 (2016).
153. Ross, G. G. & Roberts, R. G. Minimal supersymmetric unification predictions. *Nucl. Phys. B* **377**, 571–592 (1992).
154. Altarelli, G. The Higgs and the excessive success of the standard model. *Frascati Phys. Ser.* **58**, 102 (2014).
155. Pokorski, S. Physics beyond the standard model in hadronic collisions. *Acta Phys. Polon. B* **47**, 1767 (2016).
156. Ross, G. G. SUSY: Quo vadis? *Eur. Phys. J. C* **74**, 2699 (2014).
157. Slavich, P. et al. Higgs-mass predictions in the MSSM and beyond. Preprint at https://arxiv.org/abs/2012.15629 (2020).
158. Jegerlehner, F. The "Ether world" and elementary particles. Preprint at https://arxiv.org/abs/hep-th/9803021 (1998).
159. Bjorken, J. Emergent gauge bosons. In *Proceedings to the Workshops: What Comes Beyond The Standard Model.* Vol. 1, https://doi.org/10.2172/798927 (DOE, 2001) http://www-public.slac.stanford.edu/sciDoc/docMeta.aspx?slacPubNumber=SLAC-PUB-9063.
160. Forster, D., Nielsen, H. B. & Ninomiya, M. Dynamical stability of local gauge symmetry: creation of light from chaos. *Phys. Lett. B* **94**, 135–140 (1980).
161. Giudice, G. F. The dawn of the post-naturalness era. In *From My Vast Repertoire ...: Guido Altarelli's Legacy* (eds Levy, A., Forte, S. & Ridolfi, G.) 267–292 (World Scientific, 2019).
162. Witten, E. Symmetry and emergence. *Nat. Phys.* **14**, 116–119 (2018).
163. Bass, S. D. Emergent gauge symmetries and particle physics. *Prog. Part. Nucl. Phys.* **113**, 103756 (2020).
164. Baskaran, G. & Anderson, P. W. Gauge theory of high temperature superconductors and strongly correlated Fermi systems. *Phys. Rev. B* **37**, 580–583 (1988).
165. Sachdev, S. Topological order, emergent gauge fields, and Fermi surface reconstruction. *Rep. Prog. Phys.* **82**, 014001 (2019).
166. Affleck, I., Zou, Z., Hsu, T. & Anderson, P. W. SU (2) gauge symmetry of the large-U limit of the Hubbard model. *Phys. Rev. B* **38**, 745–747 (1988).
167. Banerjee, D. et al. Atomic quantum simulation of dynamical gauge fields coupled to fermionic matter: from string breaking to evolution after a quench. *Phys. Rev. Lett.* **109**, 175302 (2012).
168. Bañuls, M. C. et al. Simulating lattice gauge theories within quantum technologies. *Eur. Phys. J. D* **74**, 165 (2020).
169. Wetterich, C. Gauge symmetry from decoupling. *Nucl. Phys. B* **915**, 135–167 (2017).
170. Weinberg, S. Essay: half a century of the standard model. *Phys. Rev. Lett.* **121**, 220001 (2018).
171. Baha Balantekin, A. & Kayser, B. On the properties of neutrinos. *Annu. Rev. Nucl. Part. Sci.* **68**, 313–338 (2018).
172. Weinberg, S. Baryon and lepton nonconserving processes. *Phys. Rev. Lett.* **43**, 1566–1570 (1979).
173. Aghanim, N. et al. Planck 2018 results. VI. Cosmological parameters. *Astron. Astrophys.* **641**, A6 (2020).
174. Weinberg, S. The cosmological constant problem. *Rev. Mod. Phys.* **61**, 1–23 (1989).
175. Wetterich, C. The cosmon model for an asymptotically vanishing time dependent cosmological 'constant'. *Astron. Astrophys.* **301**, 321–328 (1995).
176. Sahni, V. & Starobinsky, A. A. The case for a positive cosmological lambda term. *Int. J. Mod. Phys. D* **9**, 373–444 (2000).
177. Peebles, P. J. E. & Ratra, B. The cosmological constant and dark energy. *Rev. Mod. Phys.* **75**, 559–606 (2003).
178. Copeland, E. J., Sami, M. & Tsujikawa, S. Dynamics of dark energy. *Int. J. Mod. Phys.* **D15**, 1753–1936 (2006).
179. Straumann, N. Dark energy. *Lect. Notes Phys.* **721**, 327–397 (2007).
180. Bass, S. D. The cosmological constant puzzle. *J. Phys.* **G38**, 043201 (2011).
181. Martin, J. Everything you always wanted to know about the cosmological constant problem (but were afraid to ask). *C. R. Phys.* **13**, 566–665 (2012).
182. Dvali, G. & Gomez, C. Quantum exclusion of positive cosmological constant? *Ann. Phys.* **528**, 68–73 (2016).
183. Laureijs, R. et al. Euclid definition study report. Preprint at https://arxiv.org/abs/1110.3193 (2011).
184. Altarelli, G. Neutrino 2004: concluding talk. *Nucl. Phys. Proc. Suppl.* **143**, 470–478 (2005).
185. Bass, S. D. & Krzysiak, J. The cosmological constant and Higgs mass with emergent gauge symmetries. *Acta Phys. Polon. B* **51**, 1251 (2020).
186. Bass, S. D. & Krzysiak, J. Vacuum energy with mass generation and Higgs bosons. *Phys. Lett. B* **803**, 135351 (2020).
187. Trodden, M. Electroweak baryogenesis. *Rev. Mod. Phys.* **71**, 1463–1500 (1999).
188. Morrissey, D. E. & Ramsey-Musolf, M. J. Electroweak baryogenesis. *New J. Phys.* **14**, 125003 (2012).
189. Servant, G. The serendipity of electroweak baryogenesis. *Phil. Trans. R. Soc. Lond. A* **376**, 20170124 (2018).
190. Amaro-Seoane, P. et al. Laser interferometer space antenna. Preprint at https://arxiv.org/abs/1702.00786 (2017).
191. Caprini, C. et al. Science with the space-based interferometer eLISA. II: gravitational waves from cosmological phase transitions. *J. Cosmol. Astropart. Phys.* **2016**, 04 (2016).
192. El-Neaj, Y. A. et al. AEDGE: atomic experiment for dark matter and gravity exploration in space. *EPJ Quant. Technol.* **7**, 6 (2020).
193. Bezrukov, F. L. & Shaposhnikov, M. The standard model Higgs boson as the inflaton. *Phys. Lett. B* **659**, 703–706 (2008).
194. Jegerlehner, F. Higgs inflation and the cosmological constant. *Acta Phys. Polon. B* **45**, 1215 (2014).
195. Rubio, J. Higgs inflation. *Front. Astron. Space Sci.* **5**, 50 (2019).
196. Wetterich, C. Cosmology and the fate of dilatation symmetry. *Nucl. Phys. B* **302**, 668–696 (1988).
197. Peebles, P. J. E. & Ratra, B. Cosmology with a time variable cosmological constant. *Astrophys. J. Lett.* **325**, 17 (1988).
198. Capozziello, S. & De Laurentis, M. Extended theories of gravity. *Phys. Rep.* **509**, 167–321 (2011).
199. Brüning, O. & Rossi, L. The high-luminosity Large Hadron Collider. *Nat. Rev. Phys.* **1**, 241–243 (2019).
200. Benedikt, M. & Zimmermann, F. The physics and technology of the Future Circular Collider. *Nat. Rev. Phys.* **1**, 238–240 (2019).
201. Benedikt, M., Blondel, A., Janot, P., Mangano, M. & Zimmermann, F. Future circular colliders succeeding the LHC. *Nat. Phys.* **16**, 402–407 (2020).
202. Stapnes, S. The compact linear collider. *Nat. Rev. Phys.* **1**, 235–237 (2019).
203. Sicking, E. & Ström, R. From precision physics to the energy frontier with the compact linear collider. *Nat. Phys.* **16**, 386–392 (2020).
204. Michizono, S. The international linear collider. *Nat. Rev. Phys.* **1**, 244–245 (2019).
205. Lou, X. The circular electron positron collider. *Nat. Rev. Phys.* **1**, 232–234 (2019).
206. Agostini, M., Benato, G. & Detwiler, J. Discovery probability of next-generation neutrinoless double-β decay experiments. *Phys. Rev. D* **96**, 053001 (2017).
207. Caldwell, A., Merle, A., Schulz, O. & Totzauer, M. Global Bayesian analysis of neutrino mass data. *Phys. Rev. D* **96**, 073001 (2017).
208. Kusenko, A. Are we on the brink of the Higgs abyss? *APS Phys.* **8**, 108–110 (2015).
209. Petricca, F. et al. First results on low-mass dark matter from the CRESST-III experiment. *J. Phys. Conf. Ser.* **1342**, 012076 (2020).
210. Akerib, D. et al. Results from a search for dark matter in the complete LUX exposure. *Phys. Rev. Lett.* **118**, 021303 (2017).
211. Cui, X. et al. Dark matter results from 54-ton-day exposure of PandaX-II experiment. *Phys. Rev. Lett.* **119**, 181302 (2017).
212. Aprile, E. et al. Dark matter search results from a one ton-year exposure of XENON1T. *Phys. Rev. Lett.* **121**, 111302 (2018).
213. Agnes, P. et al. Low-mass dark matter search with the DarkSide-50 experiment. *Phys. Rev. Lett.* **121**, 081307 (2018).
214. Kniehl, B. A., Pikelner, A. F. & Veretin, O. L. mr: a C++ library for the matching and running of the standard model parameters. *Comput. Phys. Commun.* **206**, 84–96 (2016).
215. Abada, A. et al. FCC physics opportunities. *Eur. Phys. J. C* **79**, 474 (2019).

Acknowledgements
None of the results presented in this review would have been possible without the diligent efforts of all the colleagues from the LHC accelerator group, the ATLAS and CMS experiments, the computing divisions, the theoretical community and many more, who all took part in this fantastic adventure at the energy frontier. Specifically, the authors thank M. Cepeda, F. Jegerlehner and J. Krzysiak for useful discussions during the preparation of this manuscript.

Author contributions
The authors contributed equally to all aspects of the article.

Competing interests
The authors declare no competing interests.

Peer review information
Nature Reviews Physics thanks Fabio Cerutti and the other, anonymous, reviewers for their contribution to the peer review of this work.

Publisher's note
Springer Nature remains neutral with regard to jurisdictional claims in published maps and institutional affiliations.